Paradox Found: Global Accounting of Lymphocyte Protein Synthesis

Mina O. Seedhom[1], Devin Dersh[1], Jaroslav Holly[1], Mariana Pavon-Eternod[1], Jiajie Wei[1], Matthew Angel[1], Lucas Shores[1], Alexandre David[2], Jefferson Santos[1], Heather D. Hickman[1], Jonathan W. Yewdell[1]

[1]Laboratory of Viral Diseases, NIAID, NIH, Bethesda MD 20892

[2]CNRS UMR-5203; INSERM U661; UM1; UM2, Institut de Génomique Fonctionnelle, Montpellier, 34094, France

Abstract

Rapid lymphocyte cell division places enormous demands on the protein synthesis machinery. Flow cytometric measurement of puromycylated ribosome-associated nascent chains after treating cells or mice with translation initiation inhibitors reveals that ribosomes in resting lymphocytes *in vitro* and *in vivo* elongate at typical rates for mammalian cells. Intriguingly, elongation rates can be increased up to 30% by activation *in vivo* or fever temperature *in vitro*. Resting and activated lymphocytes possess abundant monosome populations, most of which actively translate *in vivo,* while *in vitro,* nearly all can be stalled prior to activation. Quantitating lymphocyte protein mass and translating ribosomes reveals a paradoxically high ratio of cellular protein to ribosomes insufficient to support their rapid *in vivo* division, suggesting that the activated lymphocyte proteome *in vivo* may be generated in an unusual manner. Our findings demonstrate the importance of a global understanding of protein synthesis in lymphocytes and other rapidly dividing immune cells.

Introduction

Naïve lymphocytes are among the smallest nucleated cells in mammals – nearly devoid of cytoplasm, with few mitochondria – and have minimal metabolic activity, consistent with doubling times on the order of hundreds to thousands of days, respectively, for B cells [1,2] and T cells [3]. Within a day of activation by cognate antigen, lymphocytes begin to divide rapidly, with reported doubling times as rapid as 2 hours [4-6]. Such Jekyll and Hyde behavior requires massive induction of DNA and protein synthesis to support daughter cell production [7] as well as synthesizing large amounts of immune regulatory (e.g., cytokines) and effector molecules (*e.g.,* antibody and cytokines) [8-10].

Pioneering studies of protein synthesis regulation in lymphocytes utilizing radiolabeled amino acids on mitogen-activated human peripheral blood lymphocytes (PBLs) reported 7 to 20-fold increases in protein synthesis activity [11,12]. While this is an impressive increase, it was assumed that sufficient protein was synthesized to enable the generation of daughter cells with the same protein content as their progenitor. Moreover, radiolabeling, like all methods, is imperfect, and its accuracy as a measure of protein synthesis rates depends on assumptions that are nearly impossible to definitively verify [13]. Applying new methods to old problems is a tried-and-true method for generating new insights and discoveries.

Indeed, newer methods, including ribosome profiling [14], tRNA arrays [15], and tandem mass spectrometry [16], are revolutionizing the field of protein translation. This includes extending classical methods. Puromycin (PMY) is an aminonucleoside antibiotic that mimics tyrosine-tRNA, binding the ribosome A site and causing rapid chain termination by covalently attaching to the C-terminus of the nascent chain. PMY was first applied in classical protein synthesis studies [17], and remains a workhorse in understanding ribosomal catalysis of protein synthesis [18-21].

We developed the ribopuromycylation method (RPM) to better localize and quantify protein translation. PM uses a brief pulse of PMY to label elongating nascent chains frozen on ribosomes by treating cells with a translation elongation inhibitor. Ribosome-

bound nascent chains are then detected using a PMY-specific monoclonal antibody in fixed and permeabilized cells via standard immunofluorescence [22] or flow cytometry [23].

Here, we use RPM, and the ribosome transit assay (RTA), an extension of RPM that measures elongation rates, in conjunction with classic techniques to quantify the number and protein synthesis activity of ribosomes in resting and activated human and mouse lymphocytes. Our findings reveal novel features of lymphocyte translation as well as a discrepancy in the protein synthesis capacity of T cells with respect to their rapid *in vivo* division rates, emphasizing the importance of quantitative accounting as a reality check for our limited understanding of fundamental aspects of cell biology and immunology.

Results

Characterizing protein synthesis in human lymphocytes with flow RPM implicates widespread ribosome stalling

We first used flow RPM to compare translation in non-activated *vs.* PMA/ionomycin/IL-2-activated human lymphocyte subsets after 2 and 5 days in culture (Figure 1A). We devolved the total flow RPM signals into $CD4^+$, $CD8^+$, and B cell ($CD19^+$) subsets to follow distinct patterns of protein synthesis in each population (Supplemental Figure 1A). Comparing lymphocytes from 3 donors revealed considerable donor heterogeneity in RPM staining of day 2 activated cells and proliferation of various lymphocyte subpopulations.

We performed RPM on cells labeled with CFSE to track cell division by dye dilution (Supplemental Figure 1B). On day 2, activated cells exhibited multiple populations, with nearly all divided cells showing a high RPM signal. We also detected increased flow RPM in a subset of non-divided cells relative to the low level of staining in day 2 non-activated cells. By day 5, many cells were $CFSE^{lo}$, with the highest RPM signals exhibited by divided cells. Many divided cells exhibited near baseline RPM signals, however, consistent with their return to the resting state. Interestingly, although non-activated cells did not divide, ~50% demonstrated increased RPM staining.

We noted that the RPM signal in activated cells was only 2- to 5-fold higher than in non-activated cells. This increase is modest compared to the ~15-fold activation-induced increase in protein synthesis in original studies [11,12]. To examine this discrepancy, we incubated cells for 15 min with harringtonin (HAR) or pactamycin (PA) to block translation initiation or emetine (EME) or cycloheximide (CHX) to block elongation. Elongation inhibitors had minor effects on RPM staining of activated or resting cells (Figure 1B), as expected due to ribosome retention of nascent chains [22]. Initiation inhibitors, however, clearly discriminated between day 1 resting and activated cells. RPM signal was diminished by up to 80-90% on day 5 post-activation. Note that at the standard translation rate of 6 amino acids/sec, 15 min is sufficient time to complete translation of all but the very longest transcripts.

We repeated this experiment using day 1 resting lymphocytes to directly compare flow RPM with classical metabolic radiolabeling with [^{3}H]-Leucine ([^{3}H]-Leu) (Figure 1C).

Again, mild effects on RPM signal were observed with the translation inhibitors. By contrast, each inhibitor nearly completely blocked incorporation of [^{3}H]-Leu into proteins. We also performed a time course examining [^{3}H]-Leu incorporation compared to flow RPM signal in day 1 resting, day 1 activated, and day 5 activated human lymphocytes. Plotting the ratios between activated and non-activated cells from RPM flow vs. [^{3}H]-Leu incorporation revealed a substantial difference between the two methods (Figure 1D).

Thus, we cannot attribute the persistence of flow RPM staining in translation initiation inhibitor-treated cells to incomplete inhibition of protein synthesis. Instead, these data are consistent with a significant fraction of "stalled" ribosomes in cultured resting cells, *i.e.,* ribosomes with nascent chains that are not actively translating. Stalled ribosomes would be labeled with PMY, as originally described in neurons [24], but would not incorporate [^{3}H]-Leu, just as we observe with resting lymphocytes.

Flow RPM measures ribosome elongation rates in live cells

To extend these findings, we developed a variation of approaches that use initiation inhibitors to measure ribosome transit times by conversion of polysomes to monosomes [25] or ribosome profiling [14]. To derive a relative ribosome transit rate, we incubate cells with HAR for increasing times before shifting cells to 4°C to halt ribosome elongation prior to flow RPM processing (Figure 2A).

We validated this approach in HeLa cells whose ribosome transit times are well characterized [26]. This revealed a curve that follows one phase exponential decay (Figure 2B), with a calculated half-life to decay of 70-150 seconds. Including EME with HAR prevented decay of the RPM signal, as predicted, since EME blocks elongation while enabling (even enhancing) puromycylation [22,27].

Immunoblotting of puromycylated nascent chains validated the approach by showing a time-dependent decrease in puromycin signal and increased M_r of nascent chains after blocking initiation (Figure 2C). This is expected since nascent chains present at later time points after blocking initiation will be longer. Incubation of EME with HAR greatly retarded the loss of signal and the shift to longer puromycylated nascent chains.

We applied this RPM-based "ribosome transit assay" (RTA) to investigate translational control in human lymphocytes. Day 5 activated lymphocytes behaved similarly to HeLa cells in their RTA half-life and EME sensitivity (Figure 2D). By contrast, in day 1 resting lymphocytes, there was a limited decay in the signal. Further, the decay was similar in EME-treated cells, consistent with the idea that the flow RPM signal in day 1 resting lymphocytes predominantly represents stalled ribosomes with bound nascent chains.

To independently measure ribosome transit times in day 1 resting *vs.* activated lymphocytes, we treated cells for increasing times with HAR and then pulse-labeled with [^{3}H]-Leu (Figure 2E). This showed that both resting and activated cells demonstrated a decay half-life of ~90-100 seconds, similar to the RTA values for activated lymphocytes and HeLa cells.

Based on these findings, we conclude that:

1. A large fraction of ribosomes stalled in resting cultured lymphocytes.

2. Elongation occurs at similar rates for HeLa cells and lymphocytes, with the active ribosomes in resting lymphocytes translating at a similar rate as fully activated lymphocytes.
3. RTA provides a simple flow cytometric measure of ribosome transit rates, confirming and extending the findings of Arguello *et al.* [28] who reported a highly similar method.

Resting human lymphocytes have a dominant monosome population

Protein translation is thought to typically occur in polysomes, consisting of multiple ribosomes transiting a single mRNA [29]. Classic [30,31] and more recent studies [32] have established, however, that resting lymphocytes have few polysomes and provided evidence for active monosome translation by their stability in high salt, which dissociates non-translating ribosomes [33].

Confirming these reports, we found that a large fraction of assembled ribosomes in resting human lymphocytes fractionate as monosomes in sucrose gradients (Supplemental Figure 2A). Polysome abundance increases over two days post-activation. Treating freshly isolated human lymphocytes with CHX to freeze ribosomes [34,35] did not increase polysome recovery (Supplemental Figure 2B). These findings, coupled with our RPM/RTA measurements, indicate that stalled ribosomes are likely monosomes.

Protein Synthesis in Mouse Lymphocytes *ex vivo*

Working with human lymphocytes is problematic. Preparations between individuals vary considerably, and the manipulations required to isolate lymphocytes from donor blood, such as elutriation and Percoll gradient purification, increase the time cells spend outside their physiological environment.

Seeking a more reproducible system without the impact of potential artefactual stalling of the translation machinery, we turned to OT-I TCR transgenic mice [36]. OT-I cells are $CD8^+$ T cells specific for a defined cognate ligand (mouse K^b MHC class I molecules bound to the ovalbumin-derived SIINFEKL peptide) that can be activated *in vitro* or *in vivo*. OT-I T cells can be obtained from spleen or lymph nodes (LNs) in reasonable numbers at ~80% purity without further manipulation.

RTA analysis revealed that there was no decay in RPM signal for day 1 resting OT-I T cells, consistent with near total stalling of once-translating ribosomes, as we identified in human lymphocytes (Figure 3A, middle panel). By contrast, in freshly isolated OT-I cells, the RPM signal decays by 50%, consistent with active translation by 50% of the ribosomes. The signal decay $t_{½}$ of 40 seconds is consistent with translation of shorter than average mRNAs or stalling on partially translated mRNAs. Polysomes were a minor fraction in freshly isolated mouse lymphocytes, even when mice were pre-treated with CHX (Supplemental Figure 2C) (further addressed in the next section).

By contrast, day 2 activated *ex vivo* OT-I T cells demonstrated a 20-fold increased RPM signal relative to resting cells, a near total signal decay with a $t_{½}$ of ~70 seconds, and a preponderance of polysomes (Figure 3A, Supplemental Figure 2D). This is consistent with the large fractional engagement of ribosomes upon activation. Notably, the decay rate is faster than observed in previous conditions and intriguingly, the rate increases by ~20% at a “fever” temperature of 39.5 C° (Figure 3B). This suggests that lymphocytes

may be able to exceed the standard mammalian cell elongation rate of ~6 residues/second [37], particularly under fever conditions, when maximizing T cell protein synthesis is likely at a premium to support their anti-viral activity by rapid division and production of effector molecules.

Protein synthesis in mouse lymphocytes and innate immune cells *in vivo*

Mammalian cells evolved, of course, in mammals, not in plastic flasks nurtured by synthetic media in a 20% oxygen atmosphere. We, therefore, adapted the RTA assay to mice. To simultaneously measure resting and activated T cells, we adoptively transferred CFSE-labeled OT-I T cells into congenic B6 mice, which we infected with SIINFEKL-expressing vaccinia virus (VACV) to activate OT-I cells. We injected mice with HAR for 0-10 min, followed by PMY injection and flow RPM processing of harvested splenocytes (Figure 4A). With each mouse providing a single data point, we could generate RTA curves for non-activated host CD4 and CD8 cells as well as transferred OT-I cells activated by VACV infection (Figure 4B). These curves show that nearly all ribosomes with nascent chains in both resting and activated lymphocytes are actively elongating proteins *in vivo*.

The elongation rate *in vivo* is surprisingly slower than the *in vitro* rate. Notably, this experiment used our original protocol of PMY alone [23] (Figure 3C) since EME, the inhibitor used to stabilize puromycylated polypeptides on ribosomes *in vitro* [22] was ineffective *in vivo*. We found, however, that CHX is active *in vivo*, arresting the accumulation of puromycylated polypeptides for at least 60 min after injecting PMY (Supplemental Figure 3A). We, therefore, modified the RTA by simultaneously treating animals with CHX with PMY to determine the relative amount of ribosome-associated nascent chains *in vivo*. This enabled comparison of translation activity in various immune cell types using 15 min HAR pretreatment values to subtract the signal from stalled ribosomes. The number of translating ribosomes varies over a narrow range among resting splenic lymphocytes, NK cells, macrophages, and neutrophils (Supplemental Figure 3B).

Using this improved RPM protocol, one day after infecting mice with VACV we now measured a ~15-fold increase in translating ribosomes in activated OT-I T cells *in vivo* (Supplemental Figure 3C) as compared to the 10-fold increase we previously reported using the original protocol [23]. As cell division progressed over the next two days, the signal from translating ribosomes decreased (Supplemental Figure 3D-E). We next performed the modified RTA to measure translation rates in OT-I cells on D 2 and 3 post-infection with VACV-SIINFEKL (Figure 4C). Ribosome transit times in activated OT-I cells were now in line with the *in vitro* rates, and were ~20% faster than transit times in recipient (non-activated) T cells.

These results indicate that:

1. Monitoring accurate translation and rates *in vivo* is possible and avoids artifacts associated with *ex vivo* lymphocyte cultures.
2. Activation increases elongation rates in lymphocytes by ~20%.

Contribution of monosomes vs. polysomes to T cell translation

We next biochemically characterized translation in resting OT-I cells *in vivo* or OT-I cells activated *in vitro* by PMA/ionomycin/IL-2. We treated animals/cells with CHX/PMY, isolated ribosomes from cell lysates on sucrose gradients in monosome and polysome fractions, blotted fractions onto nitrocellulose and stained with antibodies against RPL7 or PMY. The robust PMY signal shows that, contrary to recent claims [38,39], PMY does not completely release nascent chains when ribosomes are previously exposed to CHX (Figure 5A).

After setting the puromycylation:RPL7 ratio in polysomes to 100% (assuming that all ribosomes in the polysome fraction are actively translating), we found that 33% of monosomes in resting *in vivo* OT-I T cells and 52% of monosomes in day 2 activated OT-I T cells were puromycylated. Since *in vivo* RTA indicates that there is essentially no stalling of puromycylated ribosomes (Figure 4C), these data demonstrate robust translation in T cell monosomes. Assuming equal elongation rates, ~38% and ~32% of overall translation would occur in monosomes of resting *in vivo* and activated *in vitro* cells, respectively. We note, however, that since PMY reduces the number of polysomes recovered from CHX-treated cells by 5-10%, a small fraction of translating monosomes probably derive from the polysome population.

The high fraction of monosome-based translation is surprising in activated cells. We noted that the activation protocol we used is far less effective than that published by Tan et al. [32] which includes SIINFEKL antigenic stimulation. Direct comparison of the protocols confirmed the superiority of Tan *et al.*, as shown by activation markers (CD69, CD25, CD44), cell size (measured by side scatter, which correlates well with automated diameter measurements), and cell division (Supplemental Figure 4A-B). OT-I cells activated by this protocol yielded large increases in the observed polysome fractions of activated splenocytes, or lymph-node-derived lymphocytes (Figure 5B). This was also evident during high salt fractionation conditions, where we found that 500mM was necessary to fully dissociate non-translating ribosomes compared to the often used 300mM (Supplemental Figure 5A). T cell ribosomes had quantifiable but low levels of monosomes under these high salt conditions (Supplemental Figure 5B, note that we could not obtain enough activated OT-I cells *in vivo* for these experiments).

These findings indicate that monosomes make a major contribution to translation in resting T cells but are likely to make a minor contribution in fully activated cells.

Accounting for translation in lymphocytes: measuring the protein-to-ribosome ratio

Cells need to synthesize sufficient proteins to regenerate a complete proteome each division cycle. This number will depend on the division rate, cell size, protein concentration, and protein loss due to degradation and export (secretion, release of exosomes, loss of other cellular material). To understand how the protein synthesis apparatus enables T cell doubling as rapidly as 2h *in vivo* [4], we quantitated a number of critical protein synthesis parameters in resting and activated OT-I T cells (Figure 6A). For these experiments, we used the optimized protocol for *in vitro* OT-I T cell activation [32] that greatly increased the fraction of ribosomes in polysomes on day 1 post activation.

Automated microscope measurements revealed that OT-I T cells increase in diameter from the resting state to the day 1 and day 2 activated states, with a corresponding calculated volume increase (based on spherical geometry) of ~2.9 fold (Figure 6B). To quantify protein content, we determined total tryptophan (Trp) autofluorescence of fully denatured proteins in a total cell lysate [40]. Protein content per T cell increases ~5-fold following activation (Figure 6C), from 421 million proteins per cell (assuming an average length of 472 aa and a proteome Trp content of 0.69% [40]) to 2.15 billion proteins per cell in day 2 activated cells, resulting in a net 1.7-fold increase in protein concentration (Figure 6D).

We determined the number of ribosomes per cell using a Bioanalyzer electrophoresis device to measure the amount of 18S and 28S rRNA in purified total RNA based on staining with a RNA-binding dye and utilizing a spike-in standard mRNA to control for yield loss during RNA purification (Figure 6E). The maximal number of translating ribosomes is limited by the less abundant subunit, which in all cases is the 60S subunit (typically 75-90% of the 40S subunit). 60S subunits increased both in absolute terms and per unit cell volume as T cells became activated, reaching a maximum of ~3.6 million copies per T cell following 2d *in vitro* activation from 264,000 copies in resting T cells (Figure 6F-G). These numbers are similar to those reported by Wolf *et al.* [41], but should be more accurate since Wolf *et al.* used total cellular RNA content to estimated ribosome.

Could there be a significant pool of non-functional ribosomes in the nucleus, where initial assembly occurs, and which occupies nearly 50% of the volume of resting T lymphocytes [42] and 34% of activated T cells [43]? Immunoblotting of fractionated nuclei shows that the distribution of ribosomes in lymphocytes is similar in resting and activated OT-I T cells and HeLa cells, with only a small fraction of total ribosomal subunits detected in nuclear lysates (Supplemental Figure 6).

The ratio of proteins to ribosomes is critical since it dictates the minimal time to replicate the proteome during cell division. This dropped up to 3-fold as T cells became activated (Figure 6H). Since mammalian ribosomes elongate at ~6 residues per second [14,37], we calculated the minimal time for a ribosome to recreate the proteome based on the protein/maximally assembled ribosome ratios, not accounting for protein degradation/secretion.

For HeLa cells, it would take a ribosome 19.9 h to synthesize 910 “average” proteins of 472 amino acids, reasonably close to the reported doubling time of ~24 hours. For OT-I T cells, with an *in vitro* doubling time of ~9.7 h, the calculated minimal proteome duplication time is also within shouting distance – 10.1 h by day 2. Therefore, the division rates of *in vitro* activated OT-I T cells, and HeLa cells can be approximated from the number of proteins and functional ribosomes translating a full capacity.

Paradoxical Discrepancy in OT-I Cell Division Rate and Protein Synthesis Capacity

We extended these findings to OT-I T cells *in vivo*, determining first that adoptively transferred OT-I T cells divide most rapidly between day 1 and 2 of activation during acute viral infection, with an average doubling time of 6.8 h, slowing to approximately 7.7 h by day 2 post-infection. We sorted for transferred OT-I T cells on day 2 post-infection and measured cell size, protein, and ribosome numbers (“*ex vivo* day 2” measurements in Figure 6 graphs). Cells activated *in vivo* were similar in size and protein content to *in vitro*

activated cells, but the protein-to-ribosome ratio was significantly higher than *in vitro* activated T cells due to the presence of 2.3 million *vs.* 3.6 million 60S subunits in maximally *in vitro* activated T cells.

Remarkably, the ratio of proteins to ribosomes (1017) at this juncture dictates a minimal proteome duplication time of 22.2 h, nearly 3x the measured doubling time of 7.7 h. While our RTA measurements support a higher elongation rate *in vivo* ($t_{½}$=55 sec *vs.* 70 sec in HeLa cells), the 27% increase (7.6 residues per second) does not come close to accounting for the discrepancy. Thus, a paradox: protein synthesis activity or capacity of T cells does not support their doubling times. The imbalance is far worse in a published description of *in vivo* CD8+ T cell division as rapidly as 2 h [4], assuming that the transgenic T cells studied are similar to OT-I cells.

Discussion

Lymphocytes protect jawed vertebrates against viral and cellular microbes and tumors. To counter the essentially infinite diversity of antigens expressed by pathogens, lymphocytes evolved to generate an enormous repertoire of specific antigen receptors. Hosts hope to never need the repertoire, and until a cognate antigen appears, metabolic processes, including protein synthesis, are minimized (this might also extend the life span of naive cells since the generation of DRiPs and other damaging chemical byproducts will also be minimized). Upon activation, lymphocytes can divide with yeast-like haste [4] to achieve numbers capable of exerting effective immunity. Here, we studied aspects of protein synthesis in lymphocytes, a field dormant since the pioneering studies by the Kay and Cooper laboratories in the 70's but now experiencing a renaissance [32,41,44-46].

To measure translation elongation rates *in vivo* and *in vitro*, we developed flow RTA, which is far simpler and cheaper than original [37] and recent [14,25] methods and provides information at the level of individual cells simultaneously phenotyped by standard flow cytometry markers. While this work was in progress, the Pierre lab described "SunRiSE", a nearly identical method, to measure elongation rates *in vitro*, observing similar puromycylation decay rates following HAR treatment [28]. While our findings are similar regarding the elongation rates of fibroblasts and lymphocytes, we note that our adding elongation inhibitors to the protocol (CHX or EME) increases elongation rate accuracy.

RTA revealed exciting facets of lymphocyte translation. We find that a significant fraction of *ex vivo* lymphocytes possess stalled/primed ribosomes that puromycylate nascent chains but do not transit mRNA. Graber *et al.* [24] used the original RPM protocol to show that primary neurons possess substantial numbers of stalled ribosomes, apparently to facilitate rapid translation upon synaptic signaling. Otherwise, to our knowledge, such prolonged ribosomal stalling has not been described in mammalian cells.

Our improved RTA protocol reveals the dramatic upregulation of protein synthesis by OT-I $CD8^+$ T cells activated *in vivo,* with a 15-fold increase in translation in day 1 activated OT-I T cells *vs.* resting OT-I T cells. Activated T cells divide every 6.8 h from d1 to d2 post-VACV-SIINFEKL infection. This is consistent with a prior OT-I study in mice infected with a different SIINFEKL expressing VACV [47]. Importantly, by i.v. delivery of translation inhibitors, we show that RTA can be used to measure elongation rates *in vivo*. Though

we focus on lymphocytes, *in vivo* RTA can be used to study any cell type in animals that can be analyzed *ex vivo* in suspension by flow cytometry.

Contrary to observations *in vitro*, ribosomes are not stalled in naïve mouse T cells *in vivo*, as we show via RTA analysis of non-activated T cells. Importantly, ribosome transit times were up to ~30% faster in activated cells, consistent with the idea that lymphocytes can accelerate translation to support activation and the rapid cell division that ensues. Similarly, OT-I T cells increased elongation rates *in vitro* when incubated at fever temperature (39.5 C°). While such accelerated translation may decrease translational fidelity, the impact may be lessened by the terminal nature of lymphocyte division, since the vast majority of activated cells apoptose within a week of activation.

We additionally provide initial measurements of numbers of ribosomes and their protein synthesis activity, key values in accounting for the macroeconomics of T cell protein synthesis. Of particular importance is the ratio of cellular proteins to ribosomes; in conjunction with the elongation rate, this value dictates the minimal time (*i.e*., no protein degradation or secretion) for duplicating the proteome [48]. Using the mammalian cell "speed limit" of 6 residues per second [14,37] mouse T cells do not possess sufficient ribosomes to support a 6-8 h division time, much less the 2h division time reported Yoon and Braciale [4], Even if ribosomes in *in vivo* activated T cells are translating at 7.8 residues per second, the time required to synthesize the proteome is 2.3x greater than the observed replication time (15.5 h vs. 6.8 h).

The discrepancy is further exacerbated when accounting for protein secretion and degradation of DRiPs (30% of nascent proteins) [49-52] and retirees ($t_{½}$ of ~32 h over the entire proteome [53,54]) and the presence of stalled and resting ribosomes. Together, this likely doubles the time required to synthesize the proteome.

Something is obviously wrong. T cell doubling times of 6.8 h are very likely to be accurate, as they are simple to measure and are routinely reported in mouse T cell studies. Quantitating proteins, however, is more challenging than it might seem. Where are the potential gremlins?

1. *Quantitating cellular protein*. We initially used the various dye binding assays for quantitating cellular protein content. While these assays vary notoriously for quantitating different proteins, they provide similar values for the cellular proteome. Moreover, they were in good agreement with a completely independent method based on Trp fluorescence, which we consider the gold standard for protein quantitation [40]. We use Wisniewski and Gaugaz's value for Trp abundance in the proteome (0.69%) and note that this value is nearly identical to values obtained using the abundance of Trp toted up from proteomic analysis of 11 different human tumor cell lines [55] as well as a transgenic T cell [56]. One possible source of error is the free metabolic pool of tryptophan, but this is likely to be less than 5% of protein tryptophan [57]. Another is the presence of serum proteins in cellular lysates. These are unlikely, however, to significantly contribute to our values since we fail to see FBS-derived-BSA in SDS-PAGE of total cell lysates.
2. *Quantitating Ribosomes.* We originally quantitated ribosomes using Abs specific for ribosomal proteins in immunoblots of total cell lysates with purified

ribosomes as a standard. We eventually recognized, however, that this approach is limited by potential heterogeneity in ribosome composition [58,59], as well as the presence of free pools of any given ribosomal subunit. It dawned on us that ribosomes are, in principle, simple to quantitate based on their RNA species, which account for >80% of total cellular RNA. Though we initially quantitated rRNA species on agarose gels with purified ribosomes as a standard, we believe quantitation is more accurate using a Bioanalyzer with doped-in highly purified RNA as an absolute staining standard and a control for loss during purification of samples.

3. *Ribosome Elongation Rates.* The classical value of ~6 or fewer residues per second for radiolabeling studies of cultured cells seems likely to be accurate based on ribosome profiling [14,60]. A recent ribosome profiling study extends these findings to mice, with *in vivo* elongation rates of 6.8, 5.2, and 4.4 amino acids per second for liver, kidney, and skeletal muscle, respectively [61]. Our *in vivo* RTA data demonstrate that translation elongation in *in vivo* activated T cells is 30% faster than in cultured cells and thus is likely to be ~ 7.8 residues/sec.

While one or more of these values may yet be inaccurate, we note that Wolf *et al.*'s [41] mass spectrometric-based measurements of *in vitro* T cell protein synthetic capacity supports and even exacerbates the paradox. We must therefore consider the possibility that that lymphocytes are in such a hurry to divide that they resort to the extraordinary measure of acquiring proteins from resting lymphocytes or other cell types.

There are reports that neurons acquire ribosomes from Schwann cells [62,63] and that cancer cells acquire mitochondria from immune cells [64]. Further, through trogocytosis, lymphocytes acquire cell surface molecules from other cells [65]. We are, however, proposing that lymphocytes acquire a significant fraction of their proteome, perhaps via something akin to emperipolesis or entosis [66], where cells actively enter homotypic cells and can even divide while residing inside [67].

In any event, our findings clearly indicate how much remains to be learned about basic lymphocyte cell biology and the importance of simple accounting in squaring our models of cell biology with reality.

Acknowledgments

We are grateful to Chris Nicchitta (Duke University) for purified ribosomes and Glennys Reynoso for outstanding technical assistance. This work was supported by the Division of Intramural Research, National Institute of Allergy and Infectious Diseases.

Experimental Procedures

Mice

Specific-pathogen-free C57BL/6 mice were purchased from the Jackson Laboratory or from Taconic. OT-I TCR transgenic mice were acquired from the NIAID Intramural Research Repository. All mice were housed under specific pathogen-free conditions (including murine norovirus, mouse parvovirus, and mouse hepatitis virus) and maintained on standard rodent chow and water supplied ad libitum. All animal studies were approved by and performed in accordance with the Animal Care and Use Committee of the National Institute of Allergy and Infectious Diseases. For acute infections, and to generate memory T cells, CFSE-labeled Ly5.2+ ($CD45.2^+CD45.1^-$) OT-I T cells were adoptively transferred into Ly5.1 ($CD45.1^+CD45.2^-$) mice. A subset of these mice was infected with VACV-SIINFEKL for indicated times to activate OT-I T cells, with some mice left uninfected where specified. For experiments done directly on memory OT-I T cells, assays were done 8-9 weeks after infection.

In vivo RPM, *in vivo* RPM-RTA, and relative protein translation determination

For the standard and CHX-improved *in vivo* RPM assays, mice were intravenously injected with 100µl of a 10mg/ml solution of PMY in PBS that was warmed to 37°C, or PMY, as just described with 0.34mg per mouse of CHX. After indicated times, mice were sacrificed, and organs were collected into complete RPMI on ice (Gibco RPMI supplemented with 7.5% fetal calf serum). For the *in vivo* RTA, or the CHX-improved *in vivo* RTA, mice were intravenously injected with 100µg of HAR simultaneously with 1mg of PMY, or 1mg of PMY and 0.34mg of CHX for 5 minutes (for the maximum signal) or first intravenously injected with 100µg of HAR for the times indicated before being intravenously injected with 1mg of PMY, or PMY and 0.34mg of CHX for 5 minutes. To determine relative levels of protein translation, two sets of mice were required. In the first set, mice were intravenously injected with 100µg of HAR for 15 minutes, and then intravenously injected with 1mg of PMY and 0.34mg of CHX for 5 minutes before spleens were harvested. In the second set, mice were intravenously injected simultaneously with 0.34mg of cycloheximide and 1mg of PMY for 5 minutes before spleens were harvested.

Single cell preparation from organs

Isolated organs were crushed between two frosted microscope slides, and the resultant single cell suspension was filtered through a 70µm mesh screen. The filtered single cell suspension was then centrifuged, resuspended in ACK lysing buffer (Lonza) to lyse red blood cells, centrifuged again, and resuspended in complete RPMI for counting on a Nexcelom Cellometer Vision using Trypan Blue (Lonza BioWhittaker) for live/dead cell discrimination and cell diameter measurements.

CFSE labeling

Spleens and inguinal, mediastinal, cervical, mesenteric, and popliteal lymph nodes from OT-I TCR transgenic or C57BL/6 mice were processed into a single cell suspension, red blood cells were lysed in ACK lysing buffer, and the resultant cells filtered through a 70 µM mesh screen. After two washes in PBS, cells were counted on a Nexcelom Cellometer Vision using Trypan Blue for dead cell exclusion, and cells were labeled in 5 µM CFSE (Invitrogen) in PBS at $1x10^7$ cells per ml for 18 minutes in a 37° water bath with mixing every 6 minutes. Cells were washed three times in PBS, recounted, and adoptively transferred into the indicated mice or cultured as specified.

Human lymphocyte purification and culture conditions for human and mouse lymphocytes

Elutriated human lymphocytes were from healthy anonymous donors at the NIH Clinical Center Department of Transfusion Medicine. After collection, elutriated lymphocytes were purified on a discontinuous 35-70% Percoll (Amersham Biosciences) gradient and washed once with ACK lysing buffer (Life Technologies) to remove contaminating red blood cells. For time-course experiments, purified lymphocytes were resuspended in PBS and labeled with CFSE where indicated (as described above) to enable tracking of cell division over time. Lymphocytes were plated at 1-2 x 10^6 cells/mL in RPMI: RPMI 1640 (Gibco) supplemented with 15% FCS, 25mM HEPES (Corning Cellgro), 1mM sodium pyruvate (Gibco), and 55uM BME (Gibco). Depending on the experiment, media was also supplemented with recombinant human IL-2 (BRB NCI Frederick, 25 U/mL), PMA (Sigma, 1ng/mL), and ionomycin (Sigma, 100ng/mL). For OT-I T cell cultures, PMA was added at 100ng/ml instead, and, where noted, SIINFEKL was added (100nM) for optimal activation. Lymphocytes were cultured in 6% CO_2 at 37°C and allowed to sit overnight prior to any experiments unless noted (noted as “freshly isolated”). For time-course experiments, lymphocytes were cultured for up to 5 days and resuspended in fresh media every 2 days. Cell counts, diameters, and viabilities (through Trypan blue exclusion) were made on a Nexcelom Cellometer Vision cell counter. Cell volumes were calculated assuming spherical geometry.

***In vitro* RPM and RPM staining**

For each sample, cells were resuspended at 2 x 10^7 cells per mL and 100µl transferred into 96-well round-bottom plates. When indicated, the media contained protein translation inhibitors at the following concentrations: 5µg/mL HAR (Santa Cruz Biotechnology), 25µg/mL EME (Calbiochem), 200µg/mL CHX (Sigma), 50µg/mL anisomycin (Sigma), or 10µM pactamycin (Sigma). After a 15-minute incubation at 37°C, 50µL of 3X PMY (Calbiochem) media was added (150µg/mL, for a final concentration of 50µg/mL) and the cells were incubated for an additional 5 minutes before shifting to ice and adding 100µL of cold PBS. Cells were then stained with ethidium monoazide (10µg/mL in PBS, Molecular Probes) for live/dead cell discrimination. After thorough washing, and a 10-minute incubation with heat-inactivated sera, or 2.4G2 to block Fc receptors, cell surface antigens were labeled for 30 minutes at 4°C with the following antibodies: For human lymphocyte stains, antibodies against: CD3ε PerCP-eFluor 710 (clone OKT3, eBioscience), CD19 PE (clone HIB19, eBioscience), CD45 APC-eFluor 780 (clone 2D1, eBioscience), CD4 PE-CF594 (clone RPA-T4, BD) or CD4 PE-Cy7 (clone RPA-T4, eBioscience), and CD8α BV421 (clone RPA-T8, BD). For mouse lymphocyte stains, antibodies were: CD3ε BV786 (clone 145-2C11, BD), CD4BV510 (clone RM4-5, BD), CD5 APC-R700 (clone 53-7.3, BD), CD8α PE-CF594 (clone 53-6.7, BD), CD11b PE-Cy7 (clone M1/70, eBioscience), CD19 APC-Cy7 (eBio1D3, eBioscience), CD25 BV650 (PC61, BD), CD44 BV605 (IM7, BD), CD44 eFl450 (clone IM7, eBioscience), CD45.1 APC (clone A20, eBioscience), CD45.1 eFl450 (clone A20, eBioscience), CD45.2 eFluor450 (clone 104, eBioscience), CD45.2 PE-Cy7 (clone 104, eBioscience), CD69 PerCP-Cy5.5 (clone H1.2F3, Invitrogen), γδ TCR PE (eBioGL3, GL3, eBioscience), Gr1 PE (clone RB6-8C5, BD), NK1.1 FITC (clone PK136, eBioscience), TCRβ 711 (H57-597, BD), and Vβ5.1/Vβ5.2 PE (clone MR9-4, BD). All antibodies were used at 1:150 dilution

in buffered saline supplemented with 0.1% BSA. Next, cells were simultaneously fixed and permeabilized in fix/perm buffer (1% PFA, 0.0075% digitonin in PBS) for 20 minutes at 4°C. Intracellular PMY was labeled with an anti-PMY antibody (clone 2A4) directly conjugated with Alex Fluor 647 (conjugated using the Life Technologies Protein Labeling Kit per the manufacturer's instructions) for 1 hour. Cells were thoroughly washed and resuspended in buffered saline supplemented with 0.1% BSA, flow cytometry performed on a BD LSRII or BD LSRFortessa X-20, and resulting data analyzed with FlowJo software. To gate on OT-I T $CD8^+$ T cells, setup was: singlets by FSCa and FSCw, lymphocytes by SSCa and FSCa, EMA^- (live/dead cell marker), $CD3^+CD19^-$, $CD8^+CD4^-$, $CD45.2^+CD45.1^-$, and $Vb5^+$, and activation markers as indicated. For thymocyte subsets, gating setup was singlets by FSCa and FSCw, lymphocytes by SSCa and FSCa, EMA^-, and then subsets on combinations of CD3ε, CD4, CD8α, CD19, CD25, CD44, CD69, γδ TCR, and TCRβ. For human lymphocytes, gating setup was singlets by FSCa and FSCw, lymphocytes by SSCa and FSCa, EMA-, and on subsets as indicated.

Amino acid radiolabeling

The following reagents were used for radioactive amino acid labeling: DMEM (for labeling HeLa cells) or RPMI minus leucine (RPMI without L-leucine, L-glutamine, and sodium pyruvate from MP Biomedicals, supplemented with Glutamax and 1mM sodium pyruvate) for labeling human lymphocytes with or without inhibitors and for the [^{3}H]-Leu (Perkin Elmer) ribosome transit analysis. Cells were kept at 37°C throughout the experiment and labeling. Cells were resuspended in complete RPMI at 1 x 10^7 cells/ml and 1ml was aliquoted into fresh Eppendorf tubes. Next, cells were spun at 300g for 4 minutes and pre-treated with protein translation inhibitors (concentrations as in RPM Staining above) in complete RPMI for 15 minutes. Pre-treated cells were spun at 300g for 4 minutes, resuspended in 200µL of labeling media (RPMI-Leu) containing 0.2mCi/mL [^{3}H]-Leu in the absence or presence of protein translation inhibitors as indicated. After a 5-minute labeling period, protein translation was stopped by adding 1mL of ice-cold PBS containing 200µg/mL of CHX. For all labeling experiments, after washing cells thoroughly in ice cold PBS, cells were lysed in 100µL or 200µl of 2% SDS lysis buffer (2% SDS, 50mM Tris-HCl pH 7.5, 5mM EDTA, 15U/mL DnaseI (Roche), cOmplete mini EDTA-free protease inhibitor tablet (Roche) in water) and boiled for 30-60 minutes to ensure complete lysis. Protein amounts were quantified by the DC Protein Assay (BioRad) or by tryptophan fluorescence measurements [40]. To quantify the amount of [^{3}H]-Leu incorporated into proteins, equal amounts of lysate (six replicates per condition) were spotted onto a 96-well DEAE filter mat (PerkinElmer) and the mat was dried at 60°C. The mat was then soaked in a 10% trichloroacetic (TCA) (Calbiochem) solution for 30 minutes at room temperature, washed twice in 70% ethanol, dried at 60°C, placed in a MicroBeta sample bag (PerkinElmer) with ~6mL of BetaPlate Scint (PerkinElmer), and heat sealed. Radioactivity was quantified in a 1450 MicroBeta TriLux scintillation counter. To determine the total amount of amino acid incorporated into proteins, dilutions of the [^{3}H]-Leu stock were counted and used as standards.

In vitro RPM Ribosome Transit Analysis (RTA)

RPM-RTA: For each time point, 1 x 10^6 lymphocytes were transferred to a fresh conical tube and resuspended in 250µL of the appropriate media. Cells were kept at 37°C (or

39.5°C when indicated) throughout the experiment. An equal volume of 2X inhibitor media was added to each tube at the indicated time and the tube was vortexed briefly to mix. Depending on the time course, the 2X inhibitor media contained HAR (Santa Cruz Biotechnology) at 10µg/mL (final concentration 5µg/mL), or HAR at 10µg/mL and EME (Calbiochem) at 50µg/mL (final concentrations of 5µg/mL and 25µg/mL, respectively. At the end of the time course, an equal volume (250µL) of 3X puromycin (PMY) (Calbiochem) media (150µg/mL, for a final concentration of 50µg/mL) was added to each tube and the tube was vortexed briefly to mix. Cells were incubated for 5 minutes with PMY before adding an excess of ice-cold PBS to quench the ribopuromycylation reaction. The cells were then stained for analysis by flow cytometry as described above.

[^{3}H]-Leu RTA: Cells were kept at 37°C throughout the experiment. For each time point, 30 x 10^6 lymphocytes were transferred to fresh Eppendorf tubes and resuspended in 50µL of the RPMI-Leu. 50µl of 2X inhibitor media was added to each tube and the tubes were vortexed briefly to mix. The inhibitor concentrations are as noted above. At the indicated times, an equal volume (100µL) of [^{3}H]-Leu labeling media (RPMI-Leu media and [^{3}H]-Leu in a 1:1 ratio, 0.5mCi/mL) was added and cells were labeled for 5 minutes. To stop [^{3}H]-Leu incorporation, an excess of ice-cold PBS containing 200µg/mL CHX and 1mg/mL leucine was added before placing the cells on ice. Cells were lysed and [^{3}H]-Leu incorporation quantified as described under “Amino acid radiolabeling” subsection.

Polysome profiling

A 15-45% continuous sucrose gradient was made in Thinwall polyallomer tubes (Beckman Coulter) from 15% and 45% sucrose (MP Biomedicals) solutions in gradient buffer (20mM Tris-HCl pH 7.4, 5mM $MgCl_2$, 100mM KCl, supplemented with 100µg/mL CHX (Sigma) and 10U/mL RNaseOUT (Invitrogen)). Briefly, 5mL of the 15% sucrose solution was carefully layered onto 5mL of the 45% sucrose solution, and the tube was placed horizontally at 4°C, typically overnight or for at least 2.5 hours before the experiment. For each gradient, cells were harvested and washed in cold PBS as described above. For cell lysis, cells were first swelled by adding 950µL of a cold hypotonic buffer (20mM Tris-HCl pH 7.4, 5mM $MgCl_2$, 10mM KCl, 40U/mL RNaseOUT, 0.1U/µL SuperaseIn, supplemented with Complete EDTA-free protease inhibitors (Roche)). After 10 min of cell swelling, NP-40 was added to a final concentration of 0.5%, the resultant lysate mixed, incubated on ice for 3 min, and spun at 7000 rpm for 2 min to remove nuclei. Post-nuclear lysates were then brought to 100mM KCl (or 300mM or 500mM NaCl where indicated), layered onto 15-45% continuous sucrose gradients, and spun for 100 min at 38,000rpm at 4°C in a SW41Ti rotor (Beckman Ultracentrifuge). Gradients were syringe-fractionated mechanically from the bottom up and monitored for absorbance at 254nm (Teledyne Isco) to obtain polysome profiles. When indicated, area under the curve measurements were calculated by a trapezoidal method from the resulting curves. When required by the experiment, we concentrated monosome and polysome fractions for immunoblotting. To pellet the ribosomes, we spun the pooled monosome or polysome fractions for 1 hour or O/N at 39,000 rpm at 4°C in the SW41Ti rotor on a 34% sucrose cushion. The resultant ribosome pellet was resuspended in 2% SDS extraction buffer.

Quantitating cellular proteins

We quantitated total protein in cell lysates based on Trp fluorescence [40]. Briefly, cells (1-2 million lymphocytes per 100µl) were lysed for 10-30 minutes at 95°C in a solution of 2% SDS, 0.1 M Tris-HCl, 50 mM DTT (pH 7.8) with 15U/mL DnaseI (Roche) and a cOmplete mini EDTA-free protease inhibitor tablet (Roche) added fresh. An 8M urea, 10mM Tris-HCL with 0.5mM DTT solution was freshly prepared, and 200µl added to wells of a flat-bottomed black polystyrene plate, and 2-4 µl of either cell lysates or a Trp standard solution was added to individual wells in triplicate. Fluorescence emitted at 350nm after excitation at 295nm was measured. We also compared this assay with the commercially available DC protein assay (Bio-Rad, performed according to the manufacturer's instructions), and found that the assays generated similar values.

Quantitating cellular ribosomes

After lymphocyte isolation, the PBS-washed cell pellet was dissolved in TRIzol; a spike-in mRNA standard was added at this step (CleanCap EGFP mRNA from TriLink, L-7601) to account for RNA loss during processing. RNA purification was conducted as described in the manufacturer's TRIzol protocol, with 5µg of glycogen used as carrier and the isopropanol precipitation step conducted overnight at -20ºC. The final RNA pellet was dissolved in 50µL of ultra-pure water and roughly quantified to determine appropriate range for the Agilent bioanalyzer chip. Samples, including fresh spike-in mRNA alone, were loaded and run on RNA Nano Bioanalyzer chips (Agilent RNA Nano 6000), with a 70ºC heating step and run on a 2100 Agilent Bioanalyzer. Bioanalyzer 2100 Expert software was used to determine total RNA concentration of each sample and percent area under curve of each peak (mRNA spike-in at approximately 1000 bp, 18S rRNA at around 1800 bp, 28S rRNA at around 4000 bp). The yield of the RNA prep was calculated as follows:
(mRNA spike-in standard peak from an RNA-purified sample) / (average of 2-3 standard peaks from 75ng/µL standard wells) = (fraction of RNA that remains after the purification process). We next converted the 18S and 28S ng/µL values to 'number molecules per cell' using the number of cells that originally went into the RNA purification, the RNA yield described above, and the following values: mouse 18S = 6.40E+05 g/mol; mouse 28S = 1.60E+06 g/mol; human 18S = 6.40E+05 g/mol; human 28S = 1.70E+06 g/mol.

Immunoblotting

To fractionate cells into nuclear and non-nuclear lysates, cells were either dissolved directly in 2% SDS extraction buffer at 95°C ("all" in Supplemental Figure 6) or subjected to a hypotonic lysis procedure. Cells were swelled with a buffer containing 20mM Tris-HCl pH 7.4, 2.5mM $MgCl_2$, and 10mM KCl supplemented with protease inhibitors for 10 min on ice. NP-40 was added to a final concentration of 0.5%, and the resultant lysate was mixed, incubated on ice for 3 minutes, and spun at 7000 rpm for 1 min. Non-nuclear lysates were removed and immediately dissolved in gel loading sample buffer (Life Technologies) to prevent sample degradation. Nuclei were washed gently 2x with PBS buffer containing NP-40 and protease inhibitors. Finally, nuclear proteins were extracted by dissolving pelleted nuclei in 2% SDS extraction buffer at 95°C. Equal amounts of each fraction were prepared for SDS-PAGE.

Samples were electrophoresed in 4-12% NuPAGE Bis-Tris gels (Invitrogen). Proteins were then transferred to nitrocellulose membranes (iBlot system, Novex) and membranes stained with Ponceau S and washed with PBS to confirm transfer uniformity. Next, membranes were incubated with either StartingBlock buffer (ThermoScientific) or Odyssey Blocking Buffer (Licor), followed by primary antibody prepared in StartingBlock buffer or Odyssey Blocking Buffer with 0.1% Tween-20 (Sigma). Depending on the experiment, we used the following primary antibodies: mouse anti-PMY (clone 2A4) at 6.66µg/mL; human anti-ribosomal P antigen at 1:2000 (Immunovision); rabbit anti-RPL7 at 1:1000, rabbit anti-RPL26 at 1:2000 (Bethyl); mouse anti-beta actin at 1:4000 (Licor); rabbit anti-HSP90 at 1:500 (Santa Cruz); rat anti-GRP94 at 1:1500 (Novus); rabbit anti-RPL28 at 1:500, rabbit anti-RPL6 at 1:1000, mouse anti-PDI at 1:2000 (Abcam); mouse anti-lamin A/C at 1:2000, rabbit anti-fibrillarin at 1:1000, mouse anti-RPS6 at 1:1000, rabbit anti-histone H3 at 1:2000, rabbit anti-RPL5 at 1:1000, and rabbit anti-RPS3 at 1:1000 (Cell Signaling Technology). The number of ribosomes per cell in earlier experiments was quantified by generating a standard curve using highly purified HeLa cell or canine rough microsome ribosomes (a kind gift of Chris Nicchitta, Duke University).

Membranes were washed three times in PBS + 0.1% Tween-20 (PBS-T) followed by incubation with secondary antibodies (all from Licor; used at 1:10,000) prepared in StartingBlock buffer or Odyssey Blocking Buffer. Membranes were washed 3x in PBS-T, 1x in PBS, and scanned via a Licor Odyssey CLX scanner.

FIGURE LEGENDS

Figure 1 – Stalled ribosomes in resting *ex vivo* human lymphocytes

(A) Primary human lymphocytes from three independent donors were cultured in PMA/ionomycin and IL2 (+PMA/I) or IL-2 only (-PMA/I) for up to 5 days. $CD45^+$ cells were processed for flow RPM. (B) Primary human lymphocytes were cultured *ex vivo* as indicated, followed by a 15 minute treatment with vehicle, harringtonin (HAR, 5µg/mL), pactamycin (PA, 10µM), emetine (EME, 25µg/mL), or cycloheximide (CHX, 200µg/ml). Cells were harvested, and surface and RPM staining was performed. Gated on $CD45^+$ cells. Error bars represent standard deviation of two independent experiments. (C) Radioactive amino acid incorporation (0.2 mCi/mL [^{3}H]-Leu for 5 min) or RPM (as in B) in day 1 resting human lymphocytes. Error bars represent standard deviation of two independent experiments. (D) Radioactive amino acid incorporation and RPM in resting and activated human lymphocytes. RPM MFI values (gated on $CD45^+$ cells) on the left, [^{3}H]-Leu incorporation values (cpm) in the middle, and ratios of the activated to the resting cells on the right. Each point represents a single donor; bars indicate the mean from 3-5 independent donors.

Figure 2 – RPM measures ribosome transit times in HeLa and human lymphocytes

(A) Schematic representation of the ribopuromycylation (RPM) Ribosome Transit Analysis (RTA) method. Translation initiation is blocked and the decrease in RPM is monitored by flow cytometry as the elongating ribosomes run off mRNA. (B) RPM-RTA in HeLa cells. Harringtonin (HAR, 5µg/mL) is used to inhibit new ribosome initiation; emetine (EME, 25µg/mL) is used to freeze ribosomes on mRNA; puromycin (PMY, 50µg/mL) generates RPM signal. Curve is fitted using one phase exponential decay, and ribosome transit times are expressed as RPM half-time to decay. (C) Same as B, but cells are instead lysed in the presence of MG-132 and subjected to anti-puromycin western blot analysis. (D) Representative plots of the RPM-RTA signal in resting and activated human CD45+ lymphocytes (left three panels). Far right, ribosome transit times determined from 3 independent donors. Each dot represents data from one individual donor; the horizontal bars indicate the mean. (E) Ribosome transit times as in A but determined by [^{3}H]-Leu incorporation instead of RPM. After treatment with HAR or HAR plus EME, cells were labeled for 5 minutes in 0.25mCi/mL [^{3}H]-Leu. Right panel, ribosome transit times determined by [^{3}H]-Leu incorporation from three independent donors. Each dot represents data from one individual donor; the horizontal bars indicate the mean.

Figure 3 – RPM ribosome transit analysis in OT-I T cells *in vitro*

(A) Lymphocytes from spleens and lymph nodes from transgenic OT-I mice were isolated, and either used immediately, cultured for one day in the absence of PMA/ionomycin, or cultured for 2 days in the presence of PMA/ionomycin and IL2. RPM-RTA analysis was conducted to determine ribosome transit half-lives, both with and without EME. (B) Lymphocytes from spleens and lymph nodes from transgenic OT-I mice were isolated, labeled with CFSE, and cultured in the presence of IL-2 and PMA/ionomycin (+PI) or SIINFEKL, PMA/ionomycin, and IL2 (SIIN+PI) for either 24 or 48 hours. Cells were harvested, and RPM-RTA was performed at both 37ºC and 39.5 ºC. Half-life of RPM signal by RTA is plotted; p-values determined by paired t-test analysis.

Figure 4 – Translation rates of resting and activated T cells *in vivo*

(A) Depiction of the RPM-RTA *in vivo* method. Labeled OT-I T cells are first adoptively transferred, followed by VACV-SIINFEKL infection. RTA analysis is performed by intravenous injection of HAR and PMY (+/- CHX to prevent leakiness from HAR inhibition alone). Spleens are harvested for RPM analysis on both endogenous and transferred T cells. (B) CFSE-labeled Ly5.2$^+$ (CD45.2$^+$CD45.1$^-$) OT-I T cells were adoptively transferred into Ly5.1 (CD45.1$^+$CD45.2$^-$) mice, which were then infected with VACV-SIINFEKL to activate the OT-I cells. Three days after infection, mice were intravenously injected with HAR simultaneously with PMY for 5 minutes (maximum signal), or first injected with HAR for ~110, ~275, or ~575 seconds before being injected with PMY for 5 minutes. Splenocytes from mice were harvested, surface stained for gating and activation markers as indicated, fixed and permeabilized, and stained for RPM. Gates were CFSE^{lo} OT-I CD8$^+$ T cells to measure decay in activated cells, and CD44$^-$CD8$^+$ or CD44$^-$CD4$^+$ T cells to measure decay in resting T cells. The curve was generated by fitting to a one phase exponential decay. Representative of two independent experiments, 2-4 mice per group, with the mean and standard deviation of the calculated half-life decays as indicated.

(C) RTA, with CHX modification, of adoptively transferred OT-I T cells or un-activated host $CD8^+$ T cells in mice infected for 2 or 3 days with VACV-SIINFEKL. 3-4 independent experiments combined, normalized by setting maximum background-subtracted signal to 100.

Figure 5 – Puromycylation reveals actively translating monosomes in resting and activated T cells

(A) OT-I mice were treated intravenously with CHX and PMY, and lymphocytes from the spleens and lymph nodes were isolated and subjected to polysome profiling by ultracentrifugation through 15-45% sucrose gradients (resting T cells). OT-I T cells activated *in vitro* for 2 days with PMA/ionomycin and IL2 (without cognate SIINFEKL peptide) were treated either with CHX alone (no PMY control) or CHX with PMY and subjected to polysome profiling. The indicated fractions were collected, pooled, and their ribosomes were re-isolated and dotted onto a nitrocellulose membrane for blotting with antibodies against PMY and RPL7. After subtraction of background signal from the anti-PMY antibody (middle panel), the PMY/RPL7 ratio of monosomes was expressed relative to that of polysomes, which we define as 100% translating. Representative of two independent experiments. (B) For resting T cells, OT-I mice were treated IV with CHX, and lymphocytes from the spleens or lymph nodes were isolated and lysed. For activated T cells, lymph node or splenic OT-I T cells were stimulated *in vitro* for 2 days with PMA/ionomycin, IL2, and exogenous SIINFEKL, followed by treatment with CHX for 5 minutes. For both resting and activated cells, ribosome-containing lysates were fractionated via ultracentrifugation on 15-45% sucrose gradients.

Figure 6 – T cell accounting reveals discrepancy in proteome duplication rate for activated T cells *in vivo*

(A) Measurements made to calculate *in vitro* and *in vivo* rates of T cell division. (B) Diameter measurements made by automated cell counter for the indicated cells. Day 1 and Day 2 represent *in vitro* activated OT-I T cells. (C) Protein content per cell as measured by tryptophan fluorescence of denatured lysates. (D) Protein molecules per fL, assuming an average protein length of 472 aa and average amino acid mass of 110 Da. (E) Example output from bioanalyzer method to determine number or ribosomes per cell. Total RNA is quantified and the bioanalyzer is used to determine area under the curve for 18S and 28S percentage of total RNA. Additionally, an exogenous mRNA standard is spiked into the sample prior to RNA purification to determine the percent loss in yield during the purification procedure. Combined, these methods allow for the accurate determination of total number of 18S and 28S molecules per cell. (F) Ribosomes per cell for the indicated cells. (G) Ribosome per fL for the indicated cells. (H) The protein/ribosome ratio, a representation of how many proteins a single ribosome would need to create to duplicate the proteome. (I) Discrepancy between measured and calculated rates of division for OT-I T cells activated and dividing *in vivo*.

Supplemental Figure 1 – RPM tracks translation in distinct cell populations over time

(A) Population frequency and RPM of resting D2 or D5 human lymphocytes or PMA/ionomcyin and IL2 activated D2 or D5 human lymphocytes. Left panel is the percent of $CD45^+$ cells in the indicated population, the right panel is the amount of RPM signal in each population. (B) Representative RPM flow cytometry plot gated on $CD8^+$ T cellsSimilar data was obtained from all donors.

Supplemental Figure 2 – Dominant populations of monosomes in resting human and mouse lymphocytes

(A) Primary human lymphocytes were cultured for one day in the absence of PMA/ionomycin or for up to 2 days in the presence of PMA/ionomycin and IL2, and the cells were subjected to polysome profiling. Representative of two independent experiments. (B) Freshly isolated human lymphocytes were treated with 0.1µg/mL CHX for 30 minutes prior to cell lysis and sucrose gradient centrifugation. Representative of two independent experiments. (C) C57BL/6 mice were treated IV with vehicle or CHX. After 10 min, spleens and lymph nodes were harvested, and the resulting cells subjected to polysome profiling via ultracentrifugation through 15-45% sucrose gradients. (D) Lymphocytes or hepatocytes were harvested from OT-I mice treated IV with CHX, lysed, and processed for polysome profiling. For activated cells, OT-I T cells were treated with PMA/ionomycin and IL2 for 2 days prior to CHX treatment and polysome profiling. Bottom right; quantification of the areas under the curve of free subunits, monosomes, and polysomes. Representative of two independent experiments.

Supplemental Figure 3 – RPM cell phenotyping

(A) C57BL/6 mice were treated intravenously with CHX and PMY or only PMY. After the indicated times, splenocytes were harvested, surface stained, fixed/permeabilized, and RPM staining was performed. Representative of three independent experiments, 2-3 mice per group. (B) In one set of C57BL/6 mice, HAR was intravenously injected for 15 minutes before intravenously injecting mice with PMY for 5 min. In a second set of mice, CHX and PMY were IV injected for 5 min. Splenocytes from each set of mice were harvested, surface stained, fixed, and permeabilized, and RPM staining was performed for various immune cell subsets. To determine relative amounts of ribosomes, the 'HAR then PMY' RPM signal was subtracted from the CHX+PMY RPM signal for each cell subset after flow cytometry. Representative of two independent experiments, 2-4 mice per group. (C) CFSE-labeled $Ly5.2^+$ ($CD45.2^+CD45.1^-$) OT-I cells were adoptively transferred into $Ly5.1^+$ ($CD45.1^+CD45.2^-$) mice, which were then infected with VAC-SIINFEKL. 1-3 days after infection, mice were intravenously injected with CHX simultaneously with PMY for 5 min. Splenocytes from the mice were harvested, surface stained, fixed and permeabilized, and RPM staining was performed. Representative flow cytometry plots gated on OT-I T cells. (D) Number of divisions (by CFSE dilution) of OT-I T cells 1-3 days after infection of mice with VACV-SIINFEKL. (E) Amount of translation as measured by RPM signal (with no

PMY signal subtracted) in uninfected, or one-, two-, or three-day VACV-SIINFEKL-infected mice. Representative of four independent experiments, 2-3 mice per time point.

Supplemental Figure 4 – Exogenous SIINFEKL significantly enhances OT-I T cell activation *in vitro*

(A) Maximum-normalized MFI of CD69, CD25, CD44, and side scatter (SSCa), as well as CFSE expansion index, of OT-I T cells after 1 or 2 days with PMA/ionomycin or PMA/ionomycin with exogenous SIINFEKL. IL-2 was included in all conditions. (B) Side scatter is a good proxy for cell size. SSCa MFI plotted vs cell diameter as determined by automated cell counter measurements.

Supplemental Figure 5 – Salt stability of T cell ribosomes and monosome quantification

(A) LN and splenic OT-I T cells were mixed and stimulated *in vitro* for 2 days with SIINFEKL, PMA/ionomycin, and IL2. Cells were treated with CHX for 5 minutes, lysed, and brought to either 300 or 500mM NaCl final concentration. Ribosome-containing lysates were subjected to polysome profiling via ultracentrifugation through 15-45% sucrose gradients containing either 300 or 500mM NaCl. (B) Quantification of the areas under the curve of free subunits, monosomes, and polysomes for each sample. (C) For resting T cells, OT-I mice were treated IV with CHX and lymphocytes from the spleens or LN were isolated and lysed. For activated T cells, LN and splenic OT-I T cells were mixed and stimulated *in vitro* for 2 days with SIINFEKL, PMA/ionomycin, and IL2, treated with CHX for 5 minutes, and lysed. Lysates were subjected to polysome profiling via ultracentrifugation on 15-45% sucrose gradients after bringing both lysate and sucrose gradients to a final concentration of 500mM NaCl to dissociate non-translating ribosomes. (D) Quantification of the areas under the curve of free subunits, monosomes, and polysomes in each sample. Representative of two independent experiments.

Supplemental Figure 6 – Fractionation of HeLa or T cells reveals few ribosomal components in nuclear lysates

HeLa cells, freshly isolated resting OT-I T cells, or OT-I T cells stimulated with PMA/ionomycin and IL2 *in vitro* for 2 days were either lysed directly in SDS extraction buffer (“all”) or subjected to a hypotonic lysis procedure to isolate non-nuclear lysates and nuclear lysates. Equal amounts of each fraction were subjected to immunoblotting for markers typical of the cytosol, ER, and nucleus. Antibodies against ribosomal proteins were used to determine where the majority of ribosomal proteins (and therefore ribosomes) fractionated. Controls with Abs specific for nucleolar located fibrillarin, histone H3, lamin A/C establish lack of nuclear contamination of non-nuclear fraction and with cytoplasmic located HSP90, GRP94, PDI, actin lack of cyotoplasmic contamination of nuclear fraction.

References

1. Macallan, D.C., Wallace, D.L., Zhang, Y., Ghattas, H., Asquith, B., de Lara, C., Worth, A., Panayiotakopoulos, G., Griffin, G.E., Tough, D.F., and Beverley, P.C. (2005). B-cell kinetics in humans: rapid turnover of peripheral blood memory cells. Blood *105*, 3633-3640. 10.1182/blood-2004-09-3740.

2. van Gent, R., Kater, A.P., Otto, S.A., Jaspers, A., Borghans, J.A., Vrisekoop, N., Ackermans, M.A., Ruiter, A.F., Wittebol, S., Eldering, E., et al. (2008). In vivo dynamics of stable chronic lymphocytic leukemia inversely correlate with somatic hypermutation levels and suggest no major leukemic turnover in bone marrow. Cancer research *68*, 10137-10144. 10.1158/0008-5472.CAN-08-2325.

3. Vrisekoop, N., den Braber, I., de Boer, A.B., Ruiter, A.F., Ackermans, M.T., van der Crabben, S.N., Schrijver, E.H., Spierenburg, G., Sauerwein, H.P., Hazenberg, M.D., et al. (2008). Sparse production but preferential incorporation of recently produced naive T cells in the human peripheral pool. Proc Natl Acad Sci U S A *105*, 6115-6120. 10.1073/pnas.0709713105.

4. Yoon, H., Kim, T.S., and Braciale, T.J. (2010). The cell cycle time of CD8+ T cells responding in vivo is controlled by the type of antigenic stimulus. PloS one *5*, e15423. 10.1371/journal.pone.0015423.

5. Jelley-Gibbs, D.M., Lepak, N.M., Yen, M., and Swain, S.L. (2000). Two distinct stages in the transition from naive CD4 T cells to effectors, early antigen-dependent and late cytokine-driven expansion and differentiation. Journal of immunology (Baltimore, Md. : 1950) *165*, 5017-5026.

6. Zhang, J., MacLennan, I.C., Liu, Y.J., and Lane, P.J. (1988). Is rapid proliferation in B centroblasts linked to somatic mutation in memory B cell clones? Immunol Lett *18*, 297-299.

7. Marshall, W., and Roberts, K. (1963). The growth and mitosis of human small lymphocytes after incubation with a phytohaemagglutinin. Experimental Physiology *48*, 146-155.

8. Ripps, C.S., and Hirschhorn, K. (1967). The production of immunoglobulins by human peripheral blood lymphocytes in vitro. Clin Exp Immunol *2*, 377-398.

9. Gery, I., and Waksman, B.H. (1972). Potentiation of the T-lymphocyte response to mitogens. II. The cellular source of potentiating mediator(s). J Exp Med *136*, 143-155.

10. Mier, J.W., and Gallo, R.C. (1980). Purification and some characteristics of human T-cell growth factor from phytohemagglutinin-stimulated lymphocyte-conditioned media. Proc Natl Acad Sci U S A *77*, 6134-6138.

11. Hirschhorn, K., Bach, F., Kolodny, R.L., Firschein, I.L., and Hashem, N. (1963). Immune Response and Mitosis of Human Peripheral Blood Lymphocytes in Vitro. Science *142*, 1185-1187.

12. Kay, J.E., and Korner, A. (1966). Effect of cycloheximide on protein and ribonucleic acid synthesis in cultured human lymphocytes. Biochem J *100*, 815-822.

13. Yewdell, J.W., Lacsina, J.R., Rechsteiner, M.C., and Nicchitta, C.V. (2011). Out with the old, in with the new? Comparing methods for measuring protein degradation. Cell Biol Int *35*, 457-462. CBI20110055 [pii]
10.1042/CBI20110055.

14. Ingolia, Nicholas T., Lareau, Liana F., and Weissman, Jonathan S. (2011). Ribosome Profiling of Mouse Embryonic Stem Cells Reveals the Complexity and Dynamics of Mammalian Proteomes. Cell *147*, 789-802. http://dx.doi.org/10.1016/j.cell.2011.10.002.

15. Dittmar, K.A., Goodenbour, J.M., and Pan, T. (2006). Tissue-specific differences in human transfer RNA expression. PLoS Genet *2*, e221.

16. Schwanhausser, B., Gossen, M., Dittmar, G., and Selbach, M. (2009). Global analysis of cellular protein translation by pulsed SILAC. Proteomics *9*, 205-209. 10.1002/pmic.200800275.

17. Pestka, S. (1971). Inhibitors of ribosome functions. Annual review of microbiology *25*, 487-562. 10.1146/annurev.mi.25.100171.002415.

18. Eggers, D.K., Welch, W.J., and Hansen, W.J. (1997). Complexes between nascent polypeptides and their molecular chaperones in the cytosol of mammalian cells. Mol. Biol. Cell *8*, 1559-1573.

19. Schmidt, E.K., Clavarino, G., Ceppi, M., and Pierre, P. (2009). SUnSET, a nonradioactive method to monitor protein synthesis. Nature methods *6*, 275-277. nmeth.1314 [pii]
10.1038/nmeth.1314.

20. Liu, J., Xu, Y., Stoleru, D., and Salic, A. (2012). Imaging protein synthesis in cells and tissues with an alkyne analog of puromycin. Proc Natl Acad Sci U S A *109*, 413-418. 10.1073/pnas.1111561108.

21. Nakano, K., and Hara, H. (1979). Measurement of the protein-synthetic activity in vivo of various tissues in rats by using [3H]Puromycin. Biochem J *184*, 663-668.

22. David, A., Dolan, B.P., Hickman, H.D., Knowlton, J.J., Clavarino, G., Pierre, P., Bennink, J.R., and Yewdell, J.W. (2012). Nuclear translation visualized by ribosome-bound nascent chain puromycylation. J Cell Biol *197*, 45-57. 10.1083/jcb.201112145.

23. Seedhom, M.O., Hickman, H.D., Wei, J., David, A., and Yewdell, J.W. (2016). Protein Translation Activity: A New Measure of Host Immune Cell Activation. The Journal of Immunology. 10.4049/jimmunol.1600088.

24. Graber, T.E., Hebert-Seropian, S., Khoutorsky, A., David, A., Yewdell, J.W., Lacaille, J.C., and Sossin, W.S. (2013). Reactivation of stalled polyribosomes in synaptic plasticity. Proc Natl Acad Sci U S A *110*, 16205-16210. 10.1073/pnas.1307747110.

25. Conn, C.S., and Qian, S.B. (2013). Nutrient signaling in protein homeostasis: an increase in quantity at the expense of quality. Sci Signal *6*, ra24. 10.1126/scisignal.2003520.

26. Nielsen, P.J., and McConkey, E.H. (1980). Evidence for control of protein synthesis in HeLa cells via the elongation rate. J Cell Physiol *104*, 269-281. 10.1002/jcp.1041040302.

27. David, A., Bennink, J.R., and Yewdell, J.W. (2013). Emetine optimally facilitates nascent chain puromycylation and potentiates the ribopuromycylation method (RPM) applied to inert cells. Histochemistry and cell biology *139*, 501-504. 10.1007/s00418-012-1063-8.

28. Arguello, R.J., Reverendo, M., Mendes, A., Camosseto, V., Torres, A.G., Ribas de Pouplana, L., van de Pavert, S.A., Gatti, E., and Pierre, P. (2018). SunRiSE - measuring translation elongation at single-cell resolution by means of flow cytometry. J Cell Sci *131*. 10.1242/jcs.214346.

29. Warner, J.R., Knopf, P.M., and Rich, A. (1963). A multiple ribosomal structure in protein synthesis. Proc Natl Acad Sci U S A *49*, 122-129.

30. Cooper, H.L., Berger, S.L., and Braverman, R. (1976). Free ribosomes in physiologically nondividing cells. Human peripheral lymphocytes. The Journal of biological chemistry *251*, 4891-4900.

31. Kay, J.E., Ahern, T., and Atkins, M. (1971). Control of protein synthesis during the activation of lymphocytes by phytohaemagglutinin. Biochimica et Biophysica Acta (BBA)

- Nucleic Acids and Protein Synthesis *247*, 322-334. http://dx.doi.org/10.1016/0005-2787(71)90680-0.

32. Tan, T.C.J., Knight, J., Sbarrato, T., Dudek, K., Willis, A.E., and Zamoyska, R. (2017). Suboptimal T-cell receptor signaling compromises protein translation, ribosome biogenesis, and proliferation of mouse CD8 T cells. Proc Natl Acad Sci U S A *114*, E6117-e6126. 10.1073/pnas.1700939114.

33. Zylber, E.A., and Penman, S. (1970). The effect of high ionic strength on monomers, polyribosomes, and puromycin-treated polyribosomes. Biochimica et biophysica acta *204*, 221-229.

34. Kay, J.E., Ahern, T., and Atkins, M. (1971). Control of protein synthesis during the activation of lymphocytes by phytohaemagglutinin. Biochimica et biophysica acta *247*, 322-334.

35. Stanners, C.P. (1966). The effect of cycloheximide on polyribosomes from hamster cells. Biochemical and biophysical research communications *24*, 758-764.

36. Hogquist, K.A., Jameson, S.C., Heath, W.R., Howard, J.L., Bevan, M.J., and Carbone, F.R. (1994). T cell receptor antagonist peptides induce positive selection. Cell *76*, 17-27.

37. Fan, H., and Penman, S. (1970). Regulation of protein synthesis in mammalian cells. II. Inhibition of protein synthesis at the level of initiation during mitosis. Journal of molecular biology *50*, 655-670.

38. Enam, S.U., Zinshteyn, B., Goldman, D.H., Cassani, M., Livingston, N.M., Seydoux, G., and Green, R. (2020). Puromycin reactivity does not accurately localize translation at the subcellular level. Elife *9*. 10.7554/eLife.60303.

39. Hobson, B.D., Kong, L., Hartwick, E.W., Gonzalez, R.L., and Sims, P.A. (2020). Elongation inhibitors do not prevent the release of puromycylated nascent polypeptide chains from ribosomes. eLife *9*, e60048. 10.7554/eLife.60048.

40. Wisniewski, J.R., and Gaugaz, F.Z. (2015). Fast and sensitive total protein and Peptide assays for proteomic analysis. Anal Chem *87*, 4110-4116. 10.1021/ac504689z.

41. Wolf, T., Jin, W., Zoppi, G., Vogel, I.A., Akhmedov, M., Bleck, C.K.E., Beltraminelli, T., Rieckmann, J.C., Ramirez, N.J., Benevento, M., et al. (2020). Dynamics in protein translation sustaining T cell preparedness. Nat Immunol *21*, 927-937. 10.1038/s41590-020-0714-5.

42. Petrzilka, G.E., Graf-de Beer, M., and Schroeder, H.E. (1978). Stereological model system for free cells and base-line data for human peripheral blood-derived small T-lymphocytes. Cell Tissue Res *192*, 121-142.

43. Petrzilka, G.E., and Schroeder, H.E. (1979). Activation of human T-lymphocytes. A kinetic and stereological study. Cell Tissue Res *201*, 101-127. 10.1007/bf00238051.

44. Araki, K., Morita, M., Bederman, A.G., Konieczny, B.T., Kissick, H.T., Sonenberg, N., and Ahmed, R. (2017). Translation is actively regulated during the differentiation of CD8+ effector T cells. Nature immunology *18*, 1046. 10.1038/ni.3795 https://www.nature.com/articles/ni.3795#supplementary-information.

45. Marchingo, J.M., and Cantrell, D.A. (2022). Protein synthesis, degradation, and energy metabolism in T cell immunity. Cell Mol Immunol *19*, 303-315. 10.1038/s41423-021-00792-8.

46. Howden, A.J.M., Hukelmann, J.L., Brenes, A., Spinelli, L., Sinclair, L.V., Lamond, A.I., and Cantrell, D.A. (2019). Quantitative analysis of T cell proteomes and environmental sensors during T cell differentiation. Nat Immunol *20*, 1542-1554. 10.1038/s41590-019-0495-x.

47. Xiao, Z., Curtsinger, J.M., Prlic, M., Jameson, S.C., and Mescher, M.F. (2007). The CD8 T cell response to vaccinia virus exhibits site-dependent heterogeneity of functional responses. International Immunology *19*, 733-743. 10.1093/intimm/dxm039.

48. Shore, D., and Albert, B. (2022). Ribosome biogenesis and the cellular energy economy. Curr Biol *32*, R611-r617. 10.1016/j.cub.2022.04.083.

49. Qian, S.B., Bennink, J.R., and Yewdell, J.W. (2005). Quantitating defective ribosome products. Methods in molecular biology (Clifton, N.J.) *301*, 271-281.

50. Princiotta, M.F., Finzi, D., Qian, S.B., Gibbs, J., Schuchmann, S., Buttgereit, F., Bennink, J.R., and Yewdell, J.W. (2003). Quantitating protein synthesis, degradation, and endogenous antigen processing. Immunity *18*, 343-354.

51. Schubert, U., Antón, L.C., Gibbs, J., Norbury, C.C., Yewdell, J.W., and Bennink, J.R. (2000). Rapid degradation of a large fraction of newly synthesized proteins by proteasomes. Nature *404*, 770-774. 10.1038/35008096.

52. Wheatley, D.N., Giddings, M.R., and Inglis, M.S. (1980). Kinetics of degradation of "short-" and "long-lived" proteins in cultured mammalian cells. Cell Biology International Reports *4*, 1081-1090.

53. Doherty, M.K., Hammond, D.E., Clague, M.J., Gaskell, S.J., and Beynon, R.J. (2009). Turnover of the human proteome: determination of protein intracellular stability by dynamic SILAC. Journal of proteome research *8*, 104-112.

54. Cambridge, S.B., Gnad, F., Nguyen, C., Bermejo, J.L., Krüger, M., and Mann, M. (2011). Systems-wide Proteomic Analysis in Mammalian Cells Reveals Conserved, Functional Protein Turnover. Journal of Proteome Research *10*, 5275-5284. 10.1021/pr101183k.

55. Geiger, T., Wehner, A., Schaab, C., Cox, J., and Mann, M. (2012). Comparative proteomic analysis of eleven common cell lines reveals ubiquitous but varying expression of most proteins. Molecular & Cellular Proteomics *11*, M111. 014050.

56. Hukelmann, J.L., Anderson, K.E., Sinclair, L.V., Grzes, K.M., Murillo, A.B., Hawkins, P.T., Stephens, L.R., Lamond, A.I., and Cantrell, D.A. (2016). The cytotoxic T cell proteome and its shaping by the kinase mTOR. Nat Immunol *17*, 104-112. 10.1038/ni.3314.

57. Kane, C.D., Vena, R.M., Ouellette, S.P., and Byrne, G.I. (1999). Intracellular Tryptophan Pool Sizes May Account for Differences in Gamma Interferon-Mediated Inhibition and Persistence of Chlamydial Growth in Polarized and Nonpolarized Cells. Infection and Immunity *67*, 1666-1671.

58. Genuth, N.R., and Barna, M. (2018). The Discovery of Ribosome Heterogeneity and Its Implications for Gene Regulation and Organismal Life. Mol Cell *71*, 364-374. 10.1016/j.molcel.2018.07.018.

59. Slavov, N., Semrau, S., Airoldi, E., Budnik, B., and van Oudenaarden, A. (2015). Differential stoichiometry among core ribosomal proteins. Cell reports *13*, 865-873.

60. Ingolia, N.T. (2014). Ribosome profiling: new views of translation, from single codons to genome scale. Nat Rev Genet *15*, 205-213. 10.1038/nrg3645.

61. Gerashchenko, M.V., Peterfi, Z., Yim, S.H., and Gladyshev, V.N. (2020). Translation elongation rate varies among organs and decreases with age. Nucleic Acids Research *49*, e9-e9. 10.1093/nar/gkaa1103.

62. Hendriks, W.T., MacGillavry, H.D., Alvarez, J., and van Minnen, J. (2008). Schwann cell to axon transfer of ribosomes: toward a novel understanding of the role of glia in the nervous system. The Journal of Neuroscience *28*, 11024-11029.

63. Court, F.A., Midha, R., Cisterna, B.A., Grochmal, J., Shakhbazau, A., Hendriks, W.T., and Van Minnen, J. (2011). Morphological evidence for a transport of ribosomes from Schwann cells to regenerating axons. Glia *59*, 1529-1539.

64. Saha, T., Dash, C., Jayabalan, R., Khiste, S., Kulkarni, A., Kurmi, K., Mondal, J., Majumder, P.K., Bardia, A., and Jang, H.L. (2022). Intercellular nanotubes mediate mitochondrial trafficking between cancer and immune cells. Nature nanotechnology *17*, 98-106.

65. Joly, E., and Hudrisier, D. (2003). What is trogocytosis and what is its purpose? 2. Nat.Immunol *4*, 815.

66. Yang, Y.-Q., and Li, J.-C. (2012). Progress of Research in Cell-in-Cell Phenomena. The Anatomical Record: Advances in Integrative Anatomy and Evolutionary Biology *295*, 372-377. 10.1002/ar.21537.

67. Overholtzer, M., Mailleux, A.A., Mouneimne, G., Normand, G., Schnitt, S.J., King, R.W., Cibas, E.S., and Brugge, J.S. (2007). A Nonapoptotic Cell Death Process, Entosis, that Occurs by Cell-in-Cell Invasion. Cell *131*, 966-979. http://dx.doi.org/10.1016/j.cell.2007.10.040.

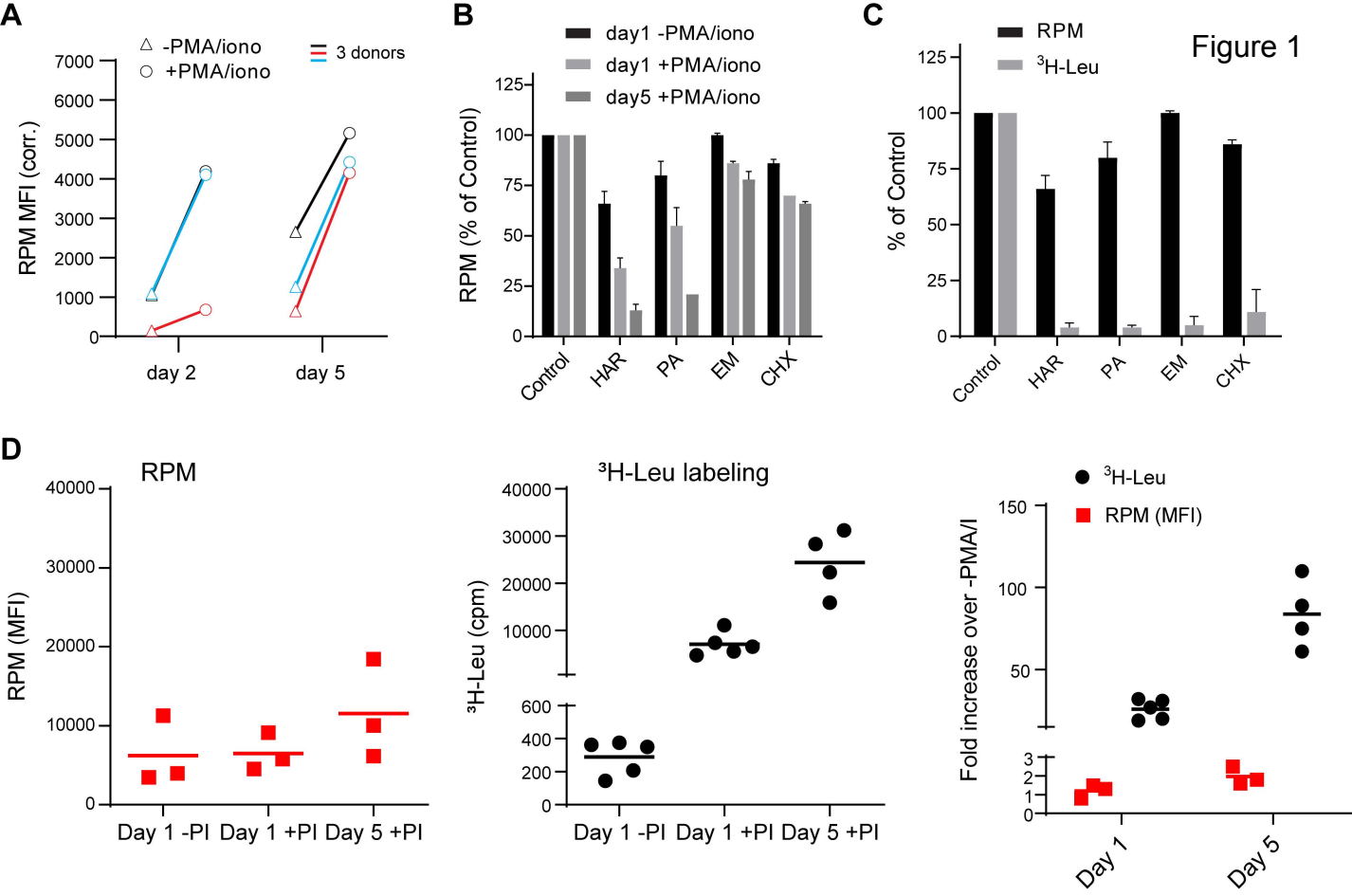
A
-PMA/iono
+PMA/iono
3 donors
RPM MFI (corr.)
7000
6000
5000
4000
3000
2000
1000
0
day 2
day 5
B
day1 -PMA/iono
day1 +PMA/iono
day5 +PMA/iono
RPM (% of Control)
125
100
75
50
25
0
Control
HAR
PA
EM
CHX
C
RPM
3H-Leu
Figure 1
% of Control
125
100
75
50
25
0
Control
HAR
PA
EM
CHX
D
RPM
RPM (MFI)
40000
30000
20000
10000
0
Day 1 -PI
Day 1 +PI
Day 5 +PI
3H-Leu labeling
3H-Leu (cpm)
40000
30000
20000
10000
600
400
200
0
Day 1 -PI
Day 1 +PI
Day 5 +PI
3H-Leu
RPM (MFI)
Fold increase over -PMA/I
150
100
50
3
2
1
0
Day 1
Day 5

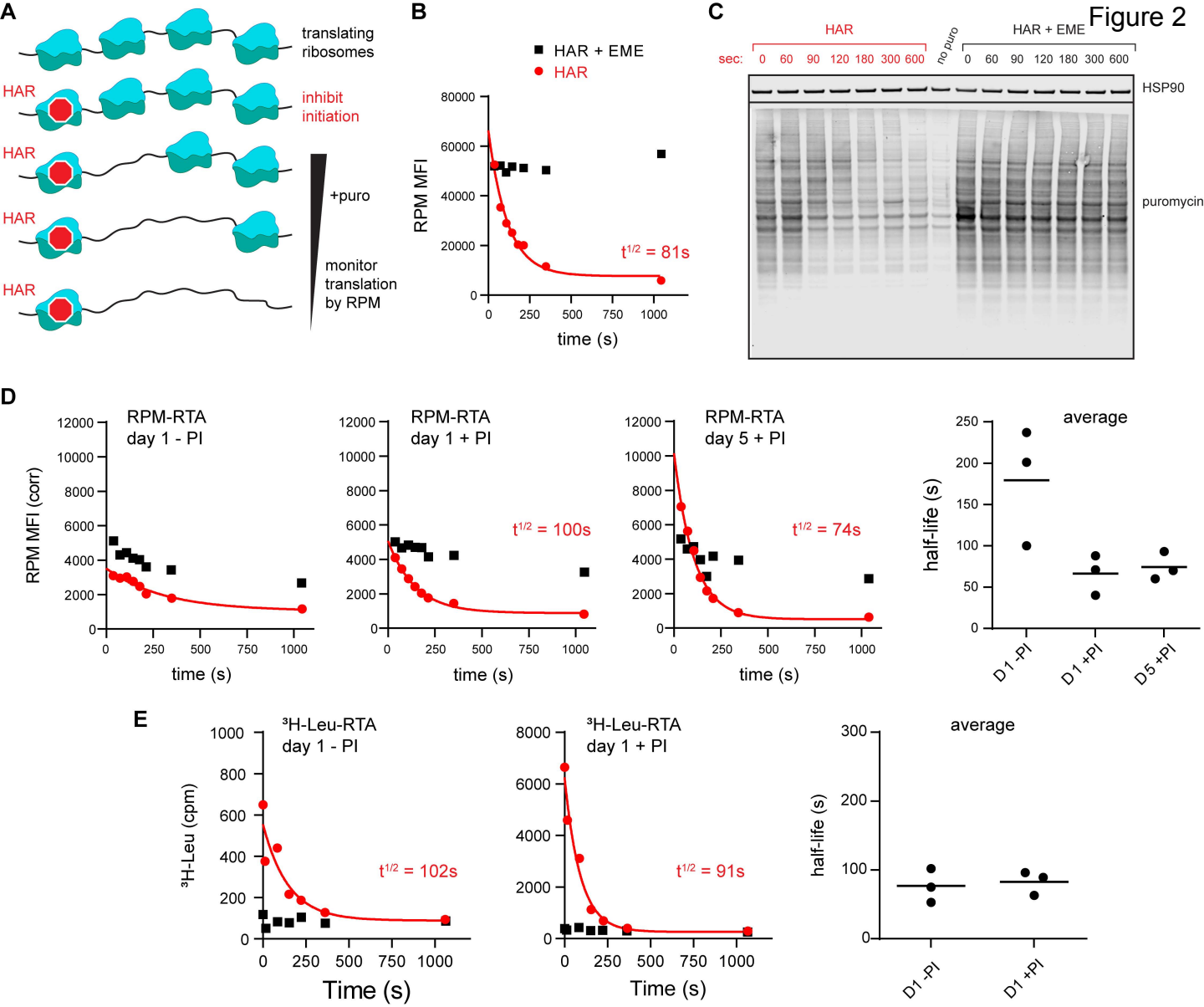
Figure 2
A
translating ribosomes
HAR
inhibit initiation
HAR
HAR
HAR
+puro
monitor translation by RPM
B
HAR + EME
HAR
RPM MFI
t1/2 = 81s
time (s)
C
HAR
HAR + EME
sec: 0 60 90 120 180 300 600
no puro
0 60 90 120 180 300 600
HSP90
puromycin
D
RPM-RTA day 1 - PI
RPM-RTA day 1 + PI
RPM-RTA day 5 + PI
RPM MFI (corr)
t1/2 = 100s
t1/2 = 74s
time (s)
average
half-life (s)
D1 -PI
D1 +PI
D5 +PI
E
3H-Leu-RTA day 1 - PI
3H-Leu-RTA day 1 + PI
3H-Leu (cpm)
t1/2 = 102s
t1/2 = 91s
Time (s)
average
half-life (s)
D1 -PI
D1 +PI

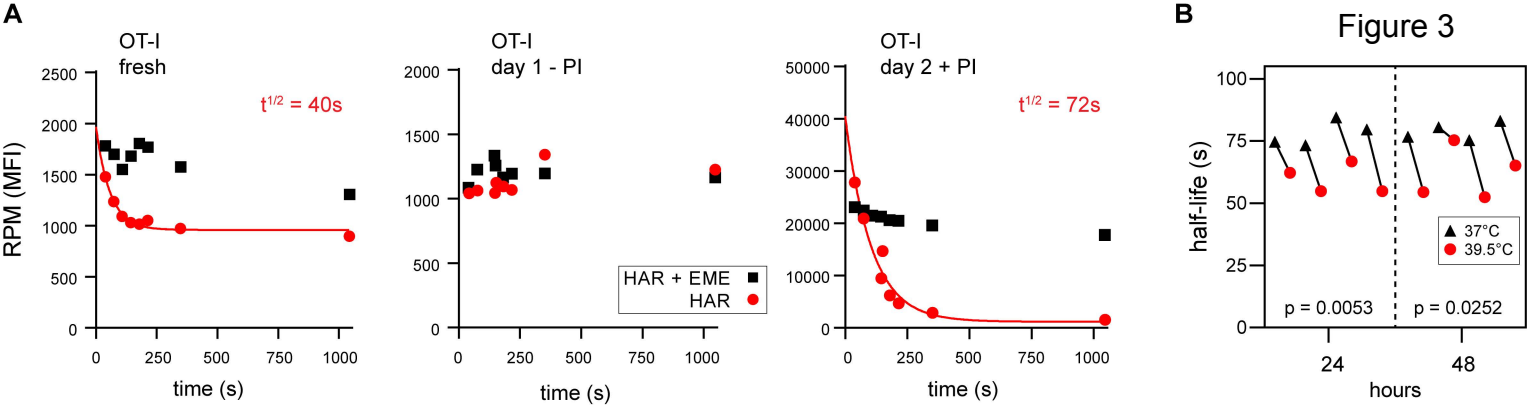
A
OT-I
fresh
$t^{1/2}$ = 40s
RPM (MFI)
time (s)
OT-I
day 1 - PI
HAR + EME
HAR
time (s)
OT-I
day 2 + PI
$t^{1/2}$ = 72s
time (s)
B
Figure 3
half-life (s)
37°C
39.5°C
p = 0.0053
p = 0.0252
24
48
hours

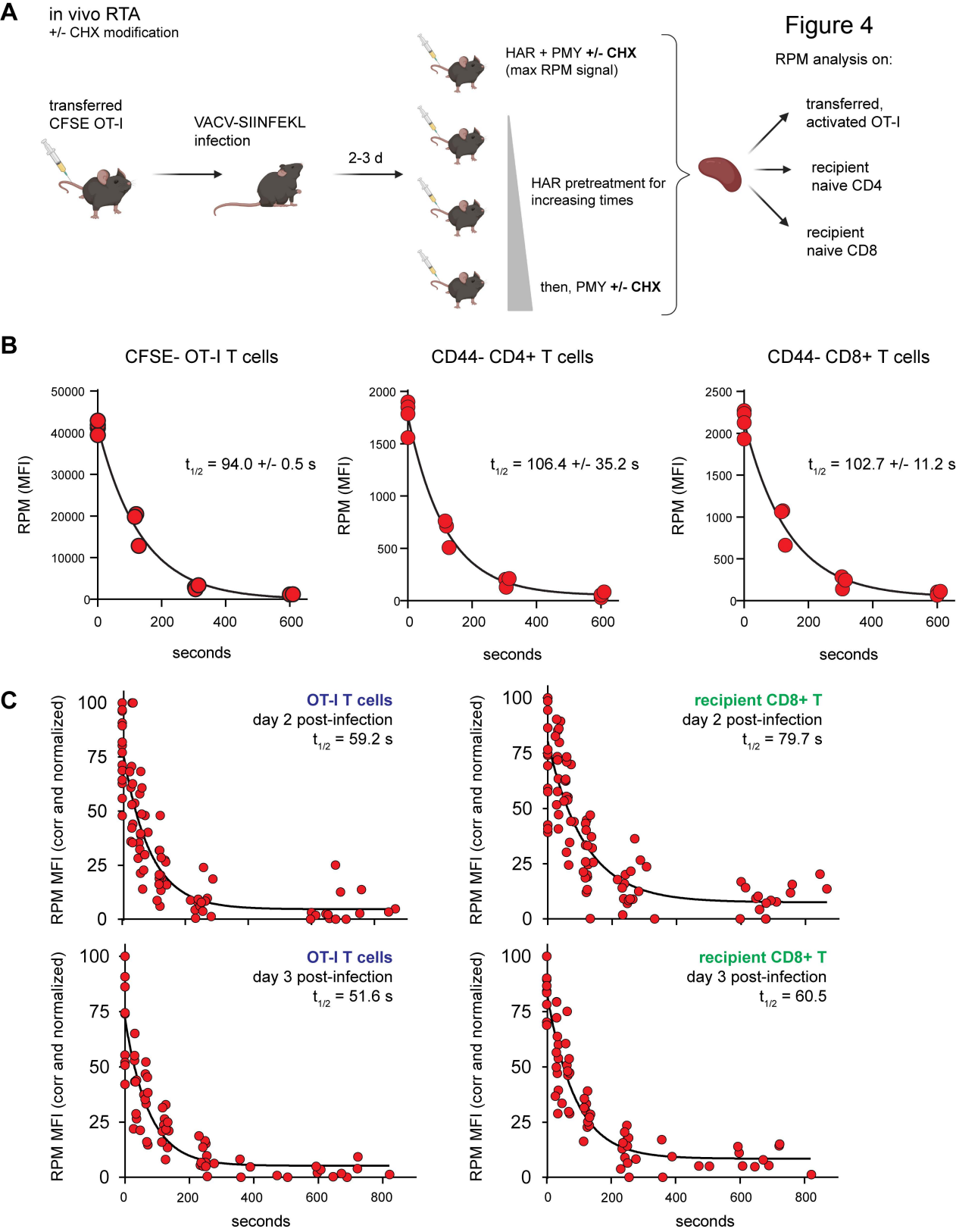

A
in vivo RTA
+/- CHX modification
Figure 4
transferred
CFSE OT-I
VACV-SIINFEKL
infection
2-3 d
HAR + PMY +/- CHX
(max RPM signal)
HAR pretreatment for
increasing times
then, PMY +/- CHX
RPM analysis on:
transferred,
activated OT-I
recipient
naive CD4
recipient
naive CD8
B
CFSE- OT-I T cells
CD44- CD4+ T cells
CD44- CD8+ T cells
RPM (MFI)
t1/2 = 94.0 +/- 0.5 s
t1/2 = 106.4 +/- 35.2 s
t1/2 = 102.7 +/- 11.2 s
seconds
C
OT-I T cells
day 2 post-infection
t1/2 = 59.2 s
recipient CD8+ T
day 2 post-infection
t1/2 = 79.7 s
OT-I T cells
day 3 post-infection
t1/2 = 51.6 s
recipient CD8+ T
day 3 post-infection
t1/2 = 60.5
RPM MFI (corr and normalized)
seconds

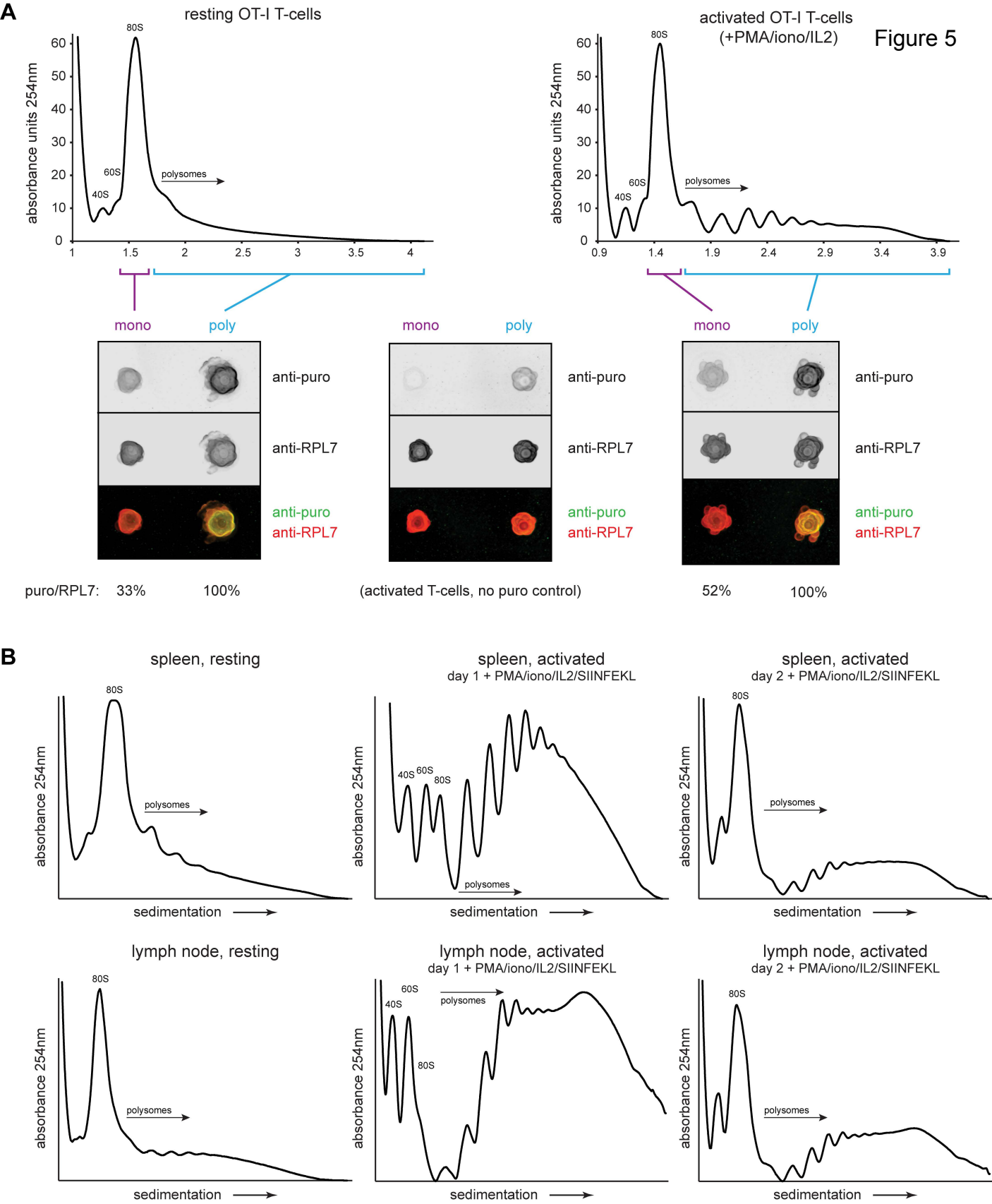
A
resting OT-I T-cells
activated OT-I T-cells
(+PMA/iono/IL2)
Figure 5
absorbance units 254nm
80S
60S
40S
polysomes
mono
poly
anti-puro
anti-RPL7
anti-puro
anti-RPL7
puro/RPL7: 33% 100%
(activated T-cells, no puro control)
52% 100%
B
spleen, resting
spleen, activated
day 1 + PMA/iono/IL2/SIINFEKL
spleen, activated
day 2 + PMA/iono/IL2/SIINFEKL
lymph node, resting
lymph node, activated
day 1 + PMA/iono/IL2/SIINFEKL
lymph node, activated
day 2 + PMA/iono/IL2/SIINFEKL
absorbance 254nm
sedimentation

Figure 6

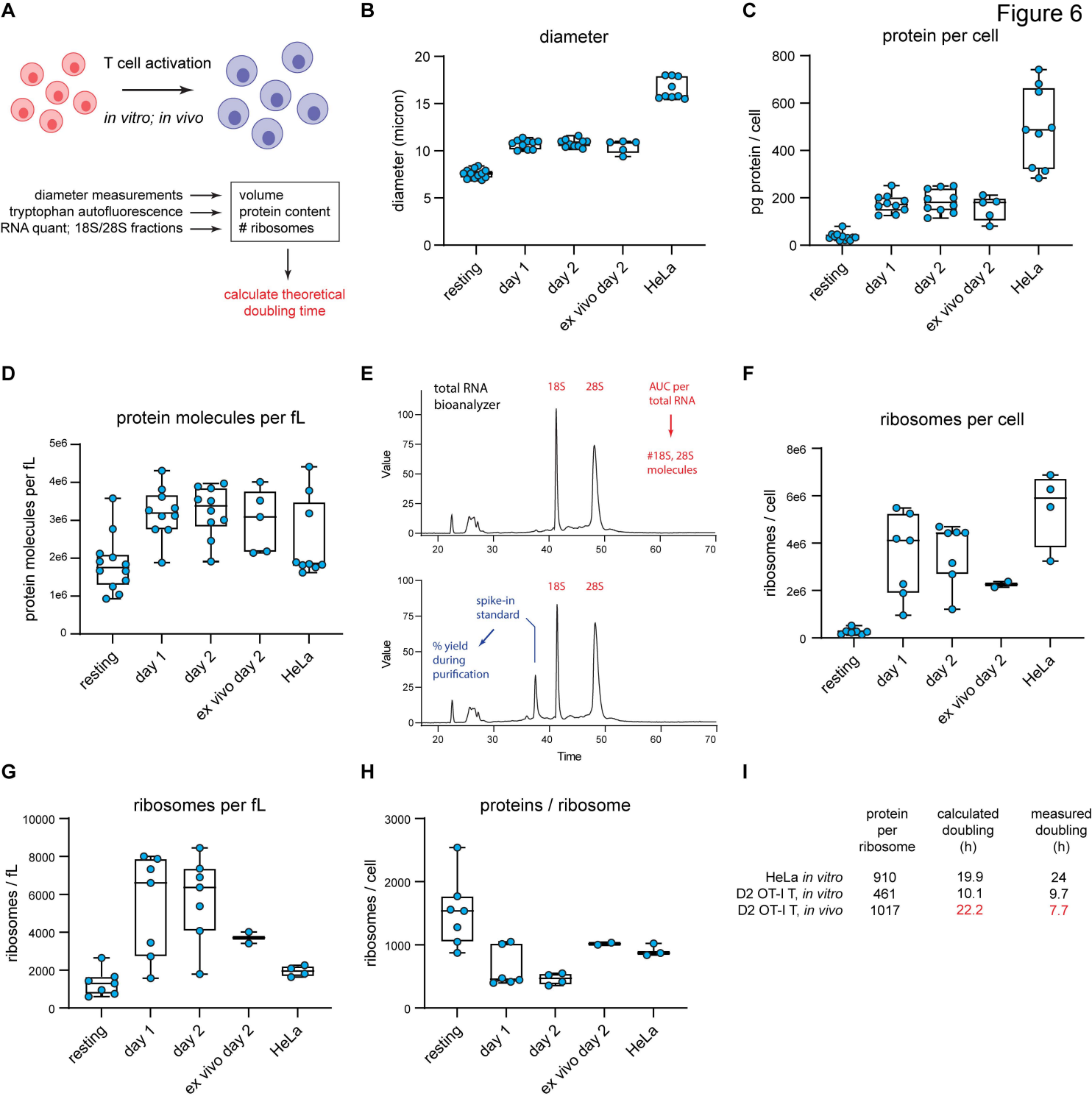

I

	protein per ribosome	calculated doubling (h)	measured doubling (h)
HeLa *in vitro*	910	19.9	24
D2 OT-I T, *in vitro*	461	10.1	9.7
D2 OT-I T, *in vivo*	1017	22.2	7.7

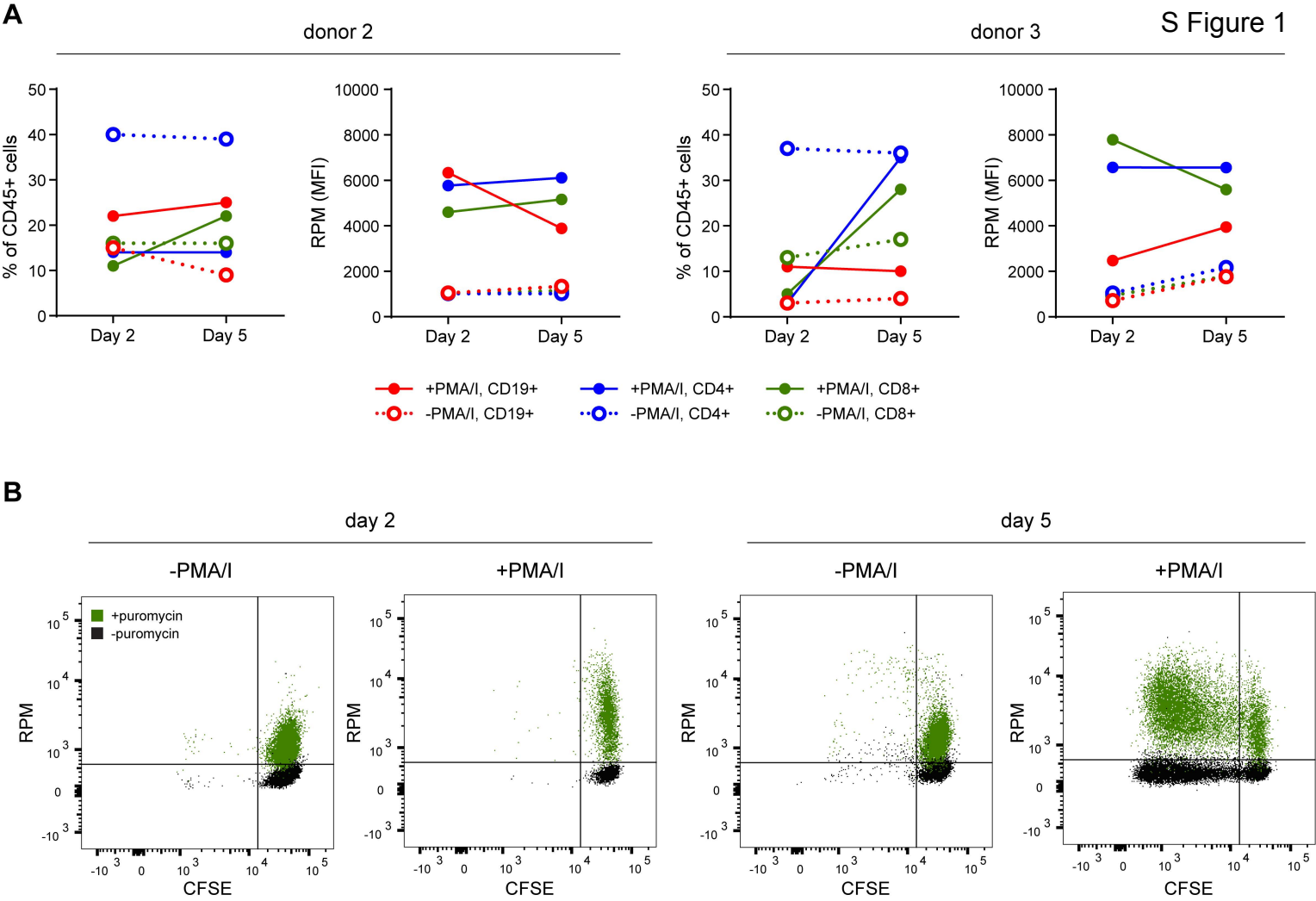
A
S Figure 1
donor 2
donor 3
% of CD45+ cells
RPM (MFI)
Day 2
Day 5
+PMA/I, CD19+
-PMA/I, CD19+
+PMA/I, CD4+
-PMA/I, CD4+
+PMA/I, CD8+
-PMA/I, CD8+
B
day 2
day 5
-PMA/I
+PMA/I
+puromycin
-puromycin
RPM
CFSE

S Figure 2

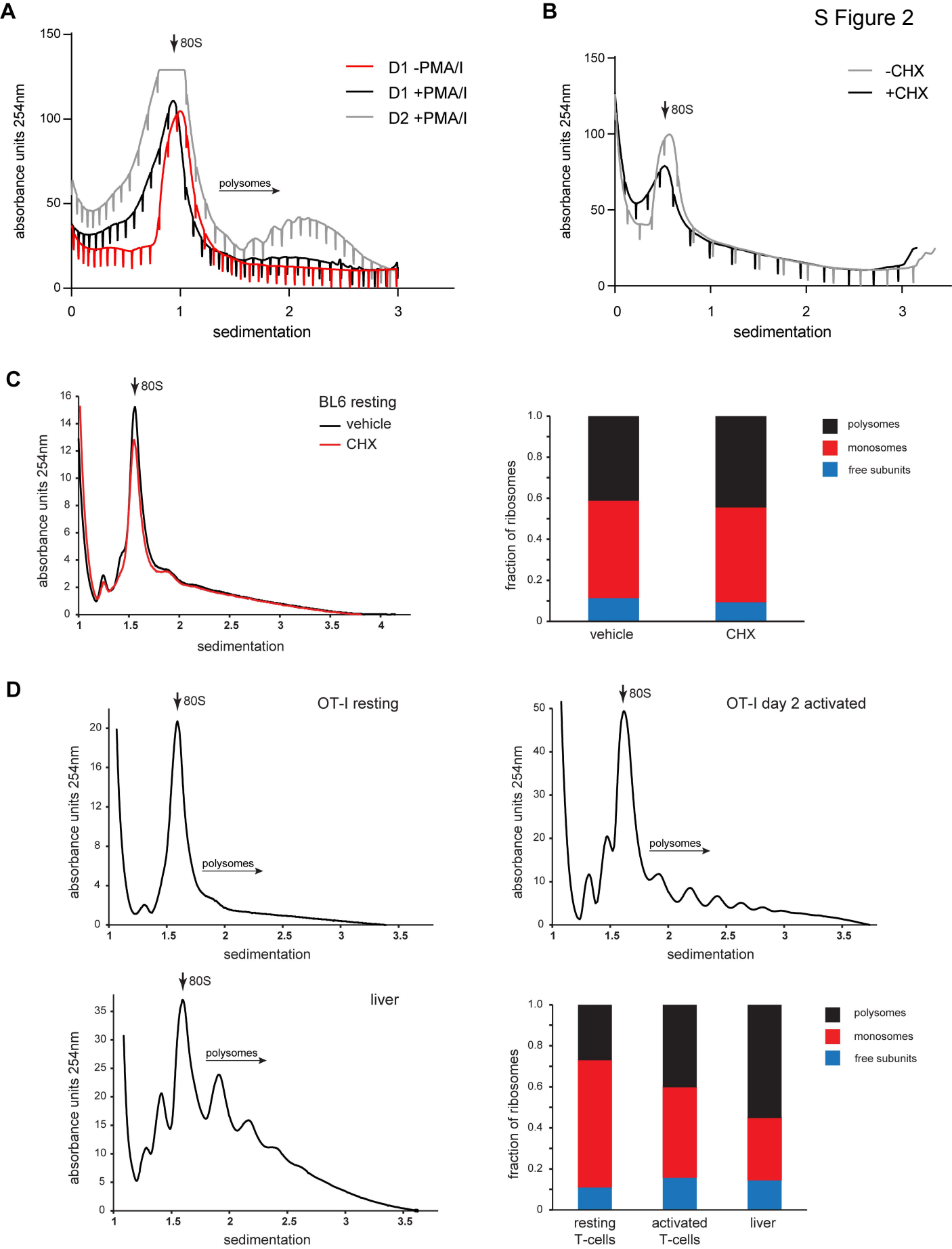
A
80S
D1 -PMA/I
D1 +PMA/I
D2 +PMA/I
polysomes
absorbance units 254nm
sedimentation
B
80S
-CHX
+CHX
absorbance units 254nm
sedimentation
C
80S
BL6 resting
vehicle
CHX
absorbance units 254nm
sedimentation
fraction of ribosomes
polysomes
monosomes
free subunits
vehicle
CHX
D
80S
OT-I resting
polysomes
absorbance units 254nm
sedimentation
80S
OT-I day 2 activated
polysomes
absorbance units 254nm
sedimentation
80S
liver
polysomes
absorbance units 254nm
sedimentation
fraction of ribosomes
polysomes
monosomes
free subunits
resting T-cells
activated T-cells
liver

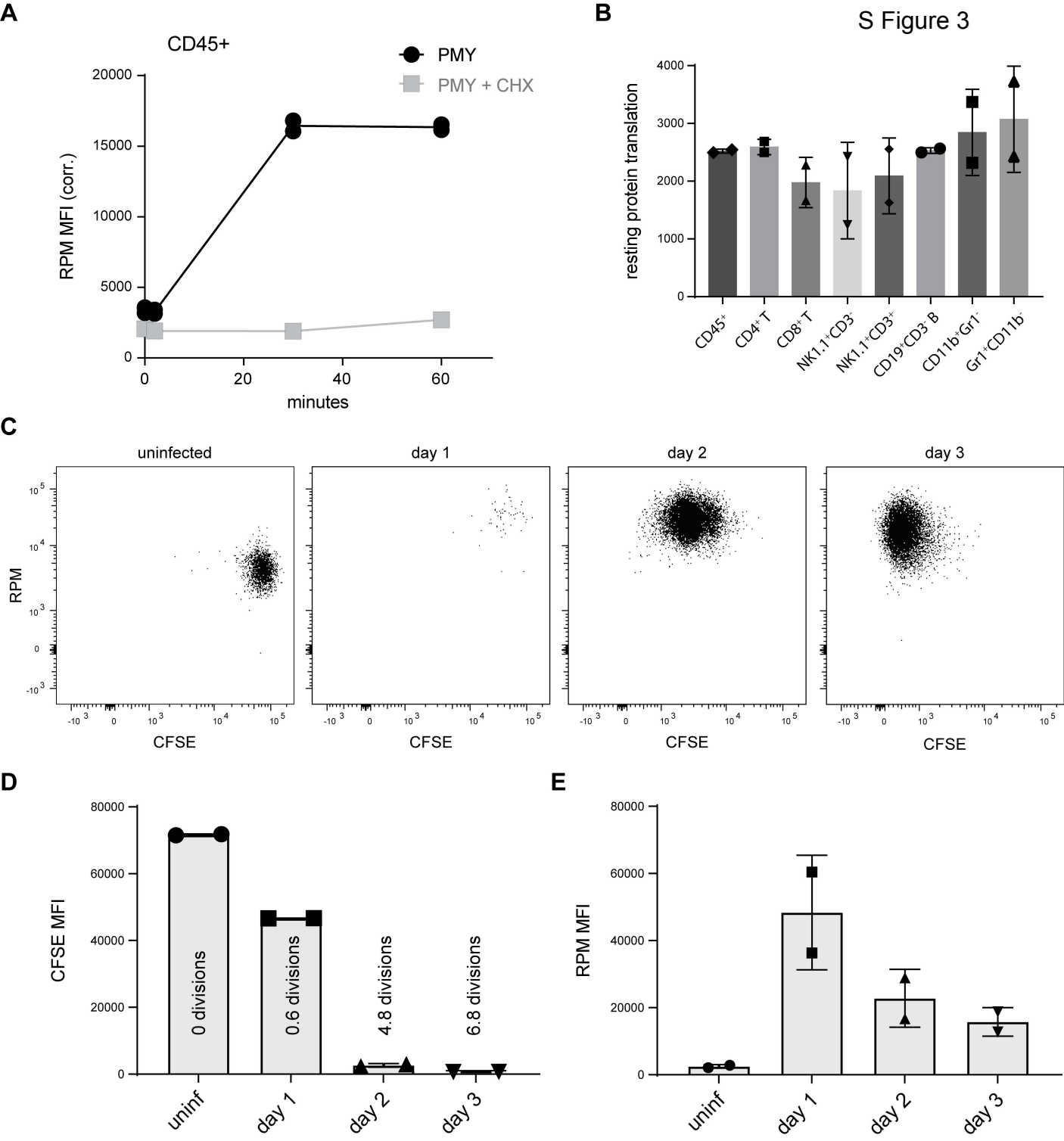
A
CD45+
PMY
PMY + CHX
RPM MFI (corr.)
minutes
B
S Figure 3
resting protein translation
CD45+
CD4+T
CD8+T
NK1.1+CD3-
NK1.1+CD3+
CD19+CD3- B
CD11b+Gr1-
Gr1+CD11b-
C
uninfected
day 1
day 2
day 3
RPM
CFSE
D
CFSE MFI
0 divisions
0.6 divisions
4.8 divisions
6.8 divisions
uninf
day 1
day 2
day 3
E
RPM MFI
uninf
day 1
day 2
day 3

S Figure 4

A

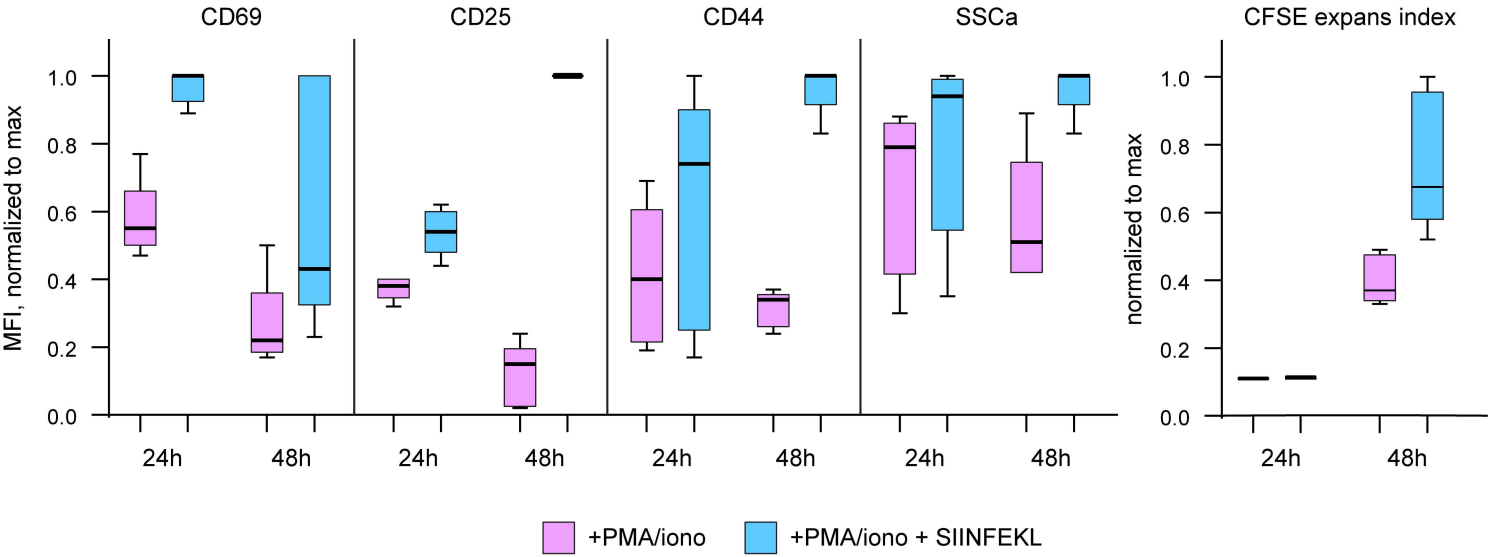
CD69
CD25
CD44
SSCa
CFSE expans index
MFI, normalized to max
normalized to max
1.0
0.8
0.6
0.4
0.2
0.0
24h
48h
+PMA/iono
+PMA/iono + SIINFEKL

B

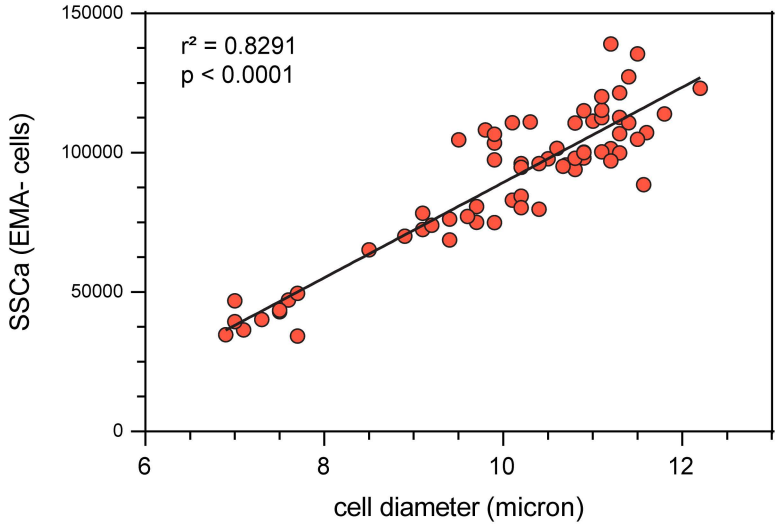
r² = 0.8291
p < 0.0001
SSCa (EMA- cells)
150000
100000
50000
0
6
8
10
12
cell diameter (micron)

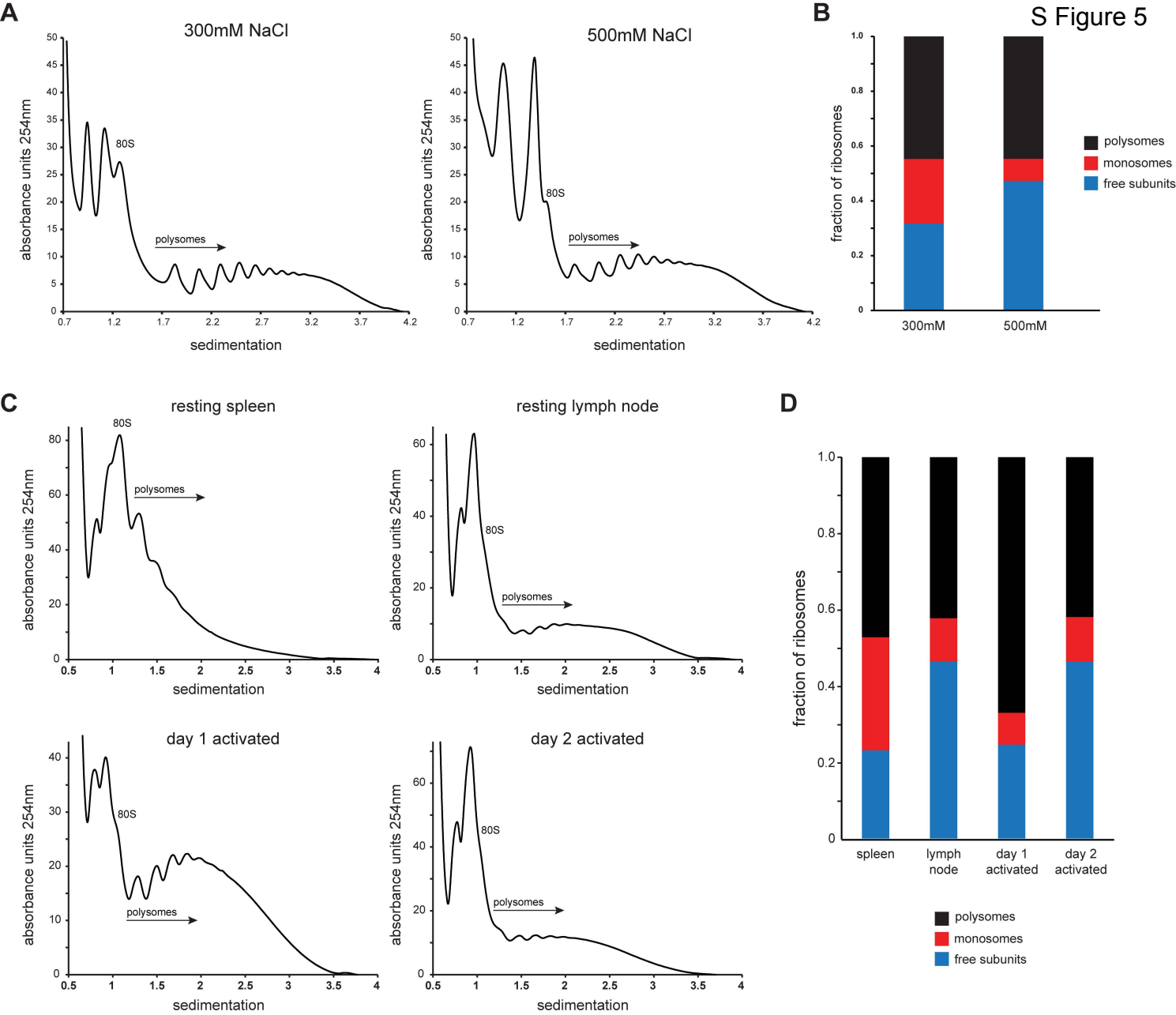
S Figure 5
A
300mM NaCl
500mM NaCl
absorbance units 254nm
sedimentation
80S
polysomes
B
fraction of ribosomes
300mM
500mM
polysomes
monosomes
free subunits
C
resting spleen
resting lymph node
day 1 activated
day 2 activated
D
spleen
lymph node
day 1 activated
day 2 activated

S Figure 6

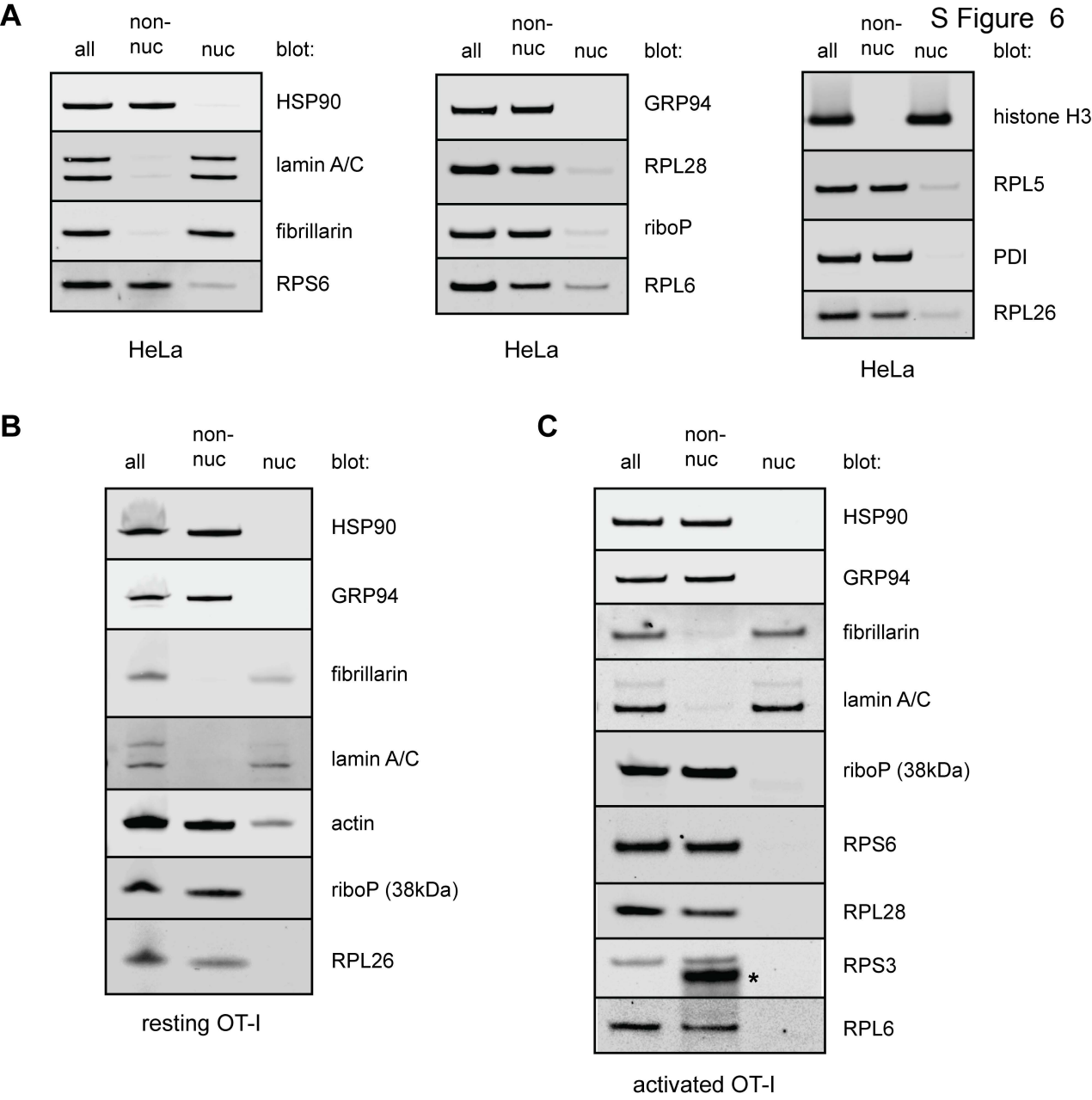
A
all
non-nuc
nuc
blot:
HSP90
lamin A/C
fibrillarin
RPS6
HeLa
all
non-nuc
nuc
blot:
GRP94
RPL28
riboP
RPL6
HeLa
all
non-nuc
nuc
blot:
histone H3
RPL5
PDI
RPL26
HeLa
B
all
non-nuc
nuc
blot:
HSP90
GRP94
fibrillarin
lamin A/C
actin
riboP (38kDa)
RPL26
resting OT-I
C
all
non-nuc
nuc
blot:
HSP90
GRP94
fibrillarin
lamin A/C
riboP (38kDa)
RPS6
RPL28
RPS3
*
RPL6
activated OT-I